

Inverse Seesaw Model with a Modular S_4 Symmetry: Lepton Flavor Mixing and Warm Dark Matter

Xinyi Zhang ^{a, 1}, Shun Zhou ^{a, b, 2}

^aInstitute of High Energy Physics, Chinese Academy of Sciences, Beijing 100049, China

^bSchool of Physical Sciences, University of Chinese Academy of Sciences, Beijing 100049, China

Abstract

In this paper, we present a systematic investigation on simple inverse seesaw models for neutrino masses and flavor mixing based on the modular S_4 symmetry. Two right-handed neutrinos and three extra fermion singlets are introduced to account for light neutrino masses through the inverse seesaw mechanism, and to provide a keV-mass sterile neutrino as the candidate for warm dark matter in our Universe. Considering all possible modular forms with weights no larger than four, we obtain twelve models, among which we find one is in excellent agreement with the observed lepton mass spectra and flavor mixing. Moreover, we explore the allowed range of the sterile neutrino mass and mixing angles, by taking into account the direct search of X -ray line and the Lyman- α observations. The model predictions for neutrino mixing parameters and the dark matter abundance will be readily testable in future neutrino oscillation experiments and cosmological observations.

¹Email: zhangxinyi@ihep.ac.cn

²Email: zhoush@ihep.ac.cn (corresponding author)

1 Introduction

Tiny but nonzero neutrino masses, as indicated by successful neutrino oscillation experiments in the past few decades [1,2], call for new physics beyond the standard model of particle physics (SM). On the other hand, cosmological observations reveal that dark matter exists in our Universe, but none of the SM particles could be the primary candidate for dark matter [3–6]. After decades of exploration, the origin of neutrino masses and the basic properties of dark matter remain mysterious, constantly attracting tremendous attention.

As for neutrino masses, the simplest explanation may be to extend the SM by introducing three right-handed neutrinos and implement the seesaw mechanism [7–9]. In this canonical type-I seesaw model, the effective mass matrix of three ordinary neutrinos is given by $M_\nu \approx -M_D M_N^{-1} M_D^T$, where the Dirac neutrino mass matrix M_D comes out from the spontaneous breakdown of electroweak gauge symmetry and thus is naturally around the electroweak scale $\Lambda_{\text{EW}} = 10^2$ GeV. Therefore, the Majorana mass matrix M_N of right-handed neutrinos is expected to be around $\Lambda_N = 10^{14}$ GeV to generate the sub-eV masses of three light neutrinos. Unfortunately, such a high-energy scale $\Lambda_N = 10^{14}$ GeV renders the type-I seesaw model impossible to be tested directly in the terrestrial collider experiments.

The inverse seesaw (ISS) mechanism [10–12] offers a possible way out of this testability problem. In the most general ISS model, there are three left-handed fermion singlets S_{iL} (for $i = 1, 2, 3$), three right-handed neutrinos N_{iR} (for $i = 1, 2, 3$), and one scalar singlet Φ , in addition to the SM particles. The gauge-invariant Lagrangian for neutrino masses can be written as

$$-\mathcal{L}_\nu = \bar{\ell}_L Y_\nu \tilde{H} N_R + \bar{S}_L Y_S N_R \Phi + \frac{1}{2} \bar{S}_L \mu S_L^C + \text{h.c.} , \quad (1)$$

where ℓ_L and $\tilde{H} \equiv i\sigma^2 H^*$ are left-handed lepton and Higgs doublets, Y_ν and Y_S are 3×3 Yukawa coupling matrices, and μ is the Majorana mass matrix of S_L . After the Higgs doublet and scalar singlet acquire their vacuum expectation values (vev's), i.e., $\langle H \rangle$ and $\langle \Phi \rangle$, the gauge symmetry is spontaneously broken and we obtain the overall 9×9 neutrino mass matrix

$$\mathcal{M} = \begin{pmatrix} \mathbf{0} & M_D & \mathbf{0} \\ M_D^T & \mathbf{0} & M_S^T \\ \mathbf{0} & M_S & \mu \end{pmatrix} , \quad (2)$$

where $M_D = Y_\nu \langle H \rangle$ and $M_S = Y_S \langle \Phi \rangle$. The effective mass matrix of three ordinary neutrinos can be derived by diagonalizing the mass matrix in Eq. (2), namely,

$$M_\nu \approx -M_D M_S^{-1} \mu (M_D M_S^{-1})^T , \quad (3)$$

where $\mathcal{O}(\mu) \ll \mathcal{O}(M_D) \ll \mathcal{O}(M_S)$ has been assumed. It is straightforward to verify that $\mathcal{O}(M_\nu) \sim 0.1$ eV can be realized by setting $\mathcal{O}(\mu) \sim 1$ keV and $\mathcal{O}(M_D M_S^{-1}) \sim 10^{-2}$. Two salient features of the ISS model can be observed. First, compared to the electroweak scale $\Lambda_{\text{EW}} = 10^2$ GeV, the mass scale $\mathcal{O}(\mu) \sim 1$ keV is highly suppressed. This is reasonable according to 't Hooft's naturalness criterion [13], since the Lagrangian in Eq. (1) gains a global $U(1)$ symmetry corresponding to the lepton number if μ is vanishing. Similar to the SM leptons, both N_R and S_L can be assigned with the lepton number $L = +1$. Therefore, only the Majorana mass term of the fermion singlets, i.e., the μ term, violates the lepton number by two units. In this sense, the lightness of three ordinary neutrinos can be ascribed to the smallness of lepton number violation. However, the lepton-number-violating mass terms associated with $\bar{N}_R^C N_R$ and $\bar{\ell}_L \tilde{H} S_L^C$ are in general allowed as well. In the literature, the former case is also considered in the inverse seesaw framework, whereas

the latter refers to the linear seesaw scenario [14]. All these possibilities share two common features: (i) the lepton-number-violating terms are naturally small; (ii) the smallness of these terms suppresses the masses of ordinary neutrinos. For clarity, these lepton-number-violating mass terms are usually considered separately, as we shall do in the present work. Second, given $\mathcal{O}(M_D) \sim \Lambda_{EW} = 10^2$ GeV, we immediately obtain $\mathcal{O}(M_S) \sim 10$ TeV, implying that the mass scale of all the singlet fermions is well accessible to the large hadron colliders [15].

In the present work, we construct a minimal but viable ISS model for neutrino masses, and further incorporate the modular S_4 symmetry into the model to explain lepton flavor mixing. The motivation for such an investigation is two-fold. First, it is interesting to interpret tiny neutrino masses and provide a suitable candidate for dark matter at the same time. The ISS model with two right-handed neutrino singlets N_{iR} (for $i = 1, 2$) and three left-handed fermion singlets S_{iL} (for $i = 1, 2, 3$), which will be denoted as ISS(2,3) [16,17], serves as a perfect framework to achieve this goal. Second, although the ISS mechanism could account for tiny neutrino masses in a natural way, the flavor structures of lepton mass matrices remain unknown. Flavor symmetry has been a powerful tool in describing lepton flavor mixing. For recent reviews, see e.g., Refs. [18–20]. The lepton flavor models based on discrete flavor symmetries suffer from the problems of too many new scalar fields (called “flavons”) and the flavons’ vacuum alignments. For this reason, we implement the modular S_4 symmetry [21], where no flavons are involved and the only source of symmetry breaking is the vev of the modulus τ . Moreover, N_{iR} (for $i = 1, 2$) and S_{iL} (for $i = 1, 2, 3$) fit perfectly into the two- and three-dimensional irreducible representations of the S_4 group. In the literature, there are a lot of studies on the S_4 modular symmetry [22–29] and those on ISS models (for an incomplete list, see Refs. [16, 30–34]), but none on both. Refs. [35, 36] consider the ISS model with a modular A_4 symmetry, but three pairs of fermion singlets are introduced and thus no dark matter candidate exists.

The remaining part of this paper is organized as follows. In Sec. 2, a simple ISS model with the modular S_4 symmetry is presented. The model predictions are confronted with the global-fit results of neutrino oscillation data in Sec. 3, and the allowed regions of model parameters are obtained. Sec. 4 is devoted to the discussions about the keV-mass sterile neutrino in our model and the observational constraints from dark matter abundance, X-ray line searches and cosmological structure formation. We summarize our main conclusions in Sec. 5. The introduction to modular symmetries, the basics of the S_4 group and the block diagonalization of neutrino mass matrix are given in Appendix A, B and C, respectively.

2 ISS Models with Modular S_4 Symmetry

One of the guiding principles for model building is simplicity. As first shown in Ref. [16], two pairs of right-handed neutrino singlets N_{iR} (for $i = 1, 2$) and left-handed fermion singlets S_{iL} (for $i = 1, 2$) are sufficient and necessary to accommodate the observed neutrino mass-squared differences and lepton flavor mixing in the ISS model. In this section, we extend this minimal ISS model by an extra fermion singlet, namely, the ISS(2, 3) model. One benefit from such an extension is to provide a keV-mass sterile neutrino, which serves as the dark matter candidate. Another one is the appealing assignment of all these fermion singlets into the irreducible representations of the modular S_4 group. More explicitly, we arrange two right-handed neutrinos N_{iR} (for $i = 1, 2$) in the two-dimensional irreducible representation **2** of S_4 , while three singlet fermions S_{iL} (for $i = 1, 2, 3$) in the three-dimensional irreducible representation **3**. The lepton doublets are assigned into the three-dimensional irreducible representation **3**, and the right-handed charged leptons are arranged in one-dimensional irreducible representations **1** or **1**'.

Although it is in principle free to choose the weights of the modular forms for the Yukawa

couplings, we perform a systematic study on models with modular-form multiplets weights no larger than four for the purpose of simplicity. Furthermore, as we have mentioned before, only one lepton-number-violating term, namely, the Majorana mass term of the fermion singlets, will be discussed. Note that other lepton-number-violating mass terms are equally allowed by the modular symmetry itself, and their phenomenological implications can be analyzed in a similar way. The construction starts with the mass term of the fermion singlets, for which we have the following possibilities¹

$$\mathbf{A1} : g (SS)_1, \quad k_S = 0 ; \quad (4)$$

$$\mathbf{A2} : g (SS)_2 Y_2, \quad k_S = -1 ; \quad (5)$$

$$\mathbf{A3} : g \left[(SS)_1 Y_1^{(4)} + r_{g_1} e^{ip_{g_1}} (SS)_2 Y_2^{(4)} + r_{g_2} e^{ip_{g_2}} (SS)_3 Y_3^{(4)} \right], \quad k_S = -2 , \quad (6)$$

where Y_2 is a modular-form multiplet of weight 2, while $Y_1^{(4)}$, $Y_2^{(4)}$ and $Y_3^{(4)}$ are those of weight 4; g is a scale factor with mass dimension, and r_{g_i} and p_{g_i} (for $i = 1, 2$) are the relative magnitudes and phases of the relevant terms. Note that \mathbf{Ai} (for $i = 1, 2, 3$) refer to different cases for the weight k_S , and we list all allowed couplings with a given weight. For a general introduction to modular symmetries, see Appendix A. More details on these modular-form multiplets can be found in Appendix B. It is worth mentioning that the Majorana mass term $(SS)_{\mathbf{3}'} Y_{\mathbf{3}'}$ or $(SS)_{\mathbf{3}'} Y_{\mathbf{3}'}^{(4)}$ is not allowed, as the irreducible representation $\mathbf{3}'$ is anti-symmetric. Then the coupling between fermion singlets and right-handed neutrinos, together with the Dirac neutrino coupling, read

$$\mathbf{B1} : \Lambda (SN^C)_{\mathbf{3}'} Y_{\mathbf{3}'}, \quad k_{NC} = -2 - k_S ; \quad (7)$$

$$\mathbf{B2} : \Lambda \left[(SN^C)_{\mathbf{3}} Y_{\mathbf{3}}^{(4)} + r_{\Lambda} e^{ip_{\Lambda}} (SN^C)_{\mathbf{3}'} Y_{\mathbf{3}'}^{(4)} \right], \quad k_{NC} = -4 - k_S ; \quad (8)$$

$$\mathbf{C1} : y (LN^C)_{\mathbf{3}'} Y_{\mathbf{3}'}, \quad k_L = -2 - k_{NC} ; \quad (9)$$

$$\mathbf{C2} : y \left[(LN^C)_{\mathbf{3}} Y_{\mathbf{3}}^{(4)} + r_y e^{ip_y} (LN^C)_{\mathbf{3}'} Y_{\mathbf{3}'}^{(4)} \right], \quad k_L = -4 - k_{NC} , \quad (10)$$

where \mathbf{Bi} (for $i = 1, 2$) denote different choices of the Yukawa coupling between the fermion singlets and right-handed neutrinos, and \mathbf{Ci} (for $i = 1, 2$) stand for different Dirac neutrino couplings; Λ is a scale factor with mass dimension, y is a dimensionless coupling, and $\{r_{\Lambda}, r_y\}$ and $\{p_{\Lambda}, p_y\}$ are the relative magnitudes and phases of the two relevant terms.

In the charged lepton sector, we take the right-handed charged leptons as singlets of S_4 . To avoid any degeneracy of charged-lepton masses, we have to introduce three different modular-form triplets to make up the charged-lepton Yukawa term. The superpotential relevant for the charged lepton Yukawa interaction can be written as

$$W_l = \alpha (LE_1^C)_{\mathbf{3}'} Y_{\mathbf{3}'} H_d + \beta (LE_2^C)_{\mathbf{3}} Y_{\mathbf{3}}^{(4)} H_d + \gamma (LE_3^C)_{\mathbf{3}'} Y_{\mathbf{3}'}^{(4)} H_d , \quad (11)$$

where dimensionless couplings α, β, γ can be chosen to be real without loss of generality. Starting from the modular forms of the lowest weight, we find $Y_{\mathbf{3}'}$, $Y_{\mathbf{3}}^{(4)}$ and $Y_{\mathbf{3}'}^{(4)}$ as in Eq. (11). However, their relative places in the superpotential can be switched, which give rise to the same mass matrix and thus do not affect the final results [23].

Since only the neutrino sector has multiple possibilities, we specify a model by choosing one possible coupling in the neutrino sector and labeling it as \mathbf{AiBjCk} (for $i = 1, 2, 3$ and $j, k = 1, 2$). We have twelve models considering different combinations. The full assignments of the chiral superfields under the SM $SU(2)$ gauge symmetry and the modular S_4 symmetry are shown in

¹When promoting the fields into chiral superfields, we use the notations $S_L \rightarrow S$ and $(N_R)^C \rightarrow N^C$.

Table 1: The charge assignments of chiral superfields under the SM SU(2) gauge symmetry and the modular S_4 symmetry.

	L	H_u	H_d	E_1^C	E_2^C	E_3^C	N^C	S
SU(2)	2	2	2	1	1	1	1	1
S_4	3	1	1	1'	1	1'	2	3

Table 1. Note that once k_S is chosen, modular weights of the other fields are fixed accordingly in a model. In addition, all the five distinct irreducible representations of S_4 (i.e., **1**, **1'**, **2**, **3** and **3'**) are utilized in the model in a natural way. Given the charge assignments, one can easily write down the gauge- and modular-invariant superpotential for neutrino masses. For example, in model **A2B2C1**, we have

$$W_\nu = y (LN^C)_{\mathbf{3}'} Y_{\mathbf{3}'} H_u + \Lambda \left[(SN^C)_{\mathbf{3}} Y_{\mathbf{3}}^{(4)} + r_\Lambda e^{ip_\Lambda} (SN^C)_{\mathbf{3}'} Y_{\mathbf{3}'}^{(4)} \right] + g (SS)_{\mathbf{2}} Y_{\mathbf{2}}. \quad (12)$$

One can choose the parameter g to be real, while in general y and Λ are complex.

After breaking of the electroweak gauge symmetry and the flavor symmetry, we get the following mass matrix for the charged leptons

$$M_l = v_d \begin{pmatrix} \alpha Y_3 & -2\beta Y_2 Y_3 & 2\gamma Y_1 Y_3 \\ \alpha Y_5 & \beta(\sqrt{3}Y_1 Y_4 + Y_2 Y_5) & \gamma(\sqrt{3}Y_2 Y_4 - Y_1 Y_5) \\ \alpha Y_4 & \beta(\sqrt{3}Y_1 Y_5 + Y_2 Y_4) & \gamma(\sqrt{3}Y_2 Y_5 - Y_1 Y_4) \end{pmatrix}^*, \quad (13)$$

where $v_d = \langle H_d \rangle$ is the vev of the down-type Higgs doublet. In the neutrino sector, the singlet fermion mass term has the following structures

$$\mathbf{A1} : \mu = g^* \begin{pmatrix} 1 & 0 & 0 \\ 0 & 0 & 1 \\ 0 & 1 & 0 \end{pmatrix}^*, \quad (14)$$

$$\mathbf{A2} : \mu = g^* \begin{pmatrix} Y_1 & 0 & 0 \\ 0 & \frac{\sqrt{3}}{2}Y_2 & -\frac{1}{2}Y_1 \\ 0 & -\frac{1}{2}Y_1 & \frac{\sqrt{3}}{2}Y_2 \end{pmatrix}^*, \quad (15)$$

$$\begin{aligned} \mathbf{A3} : \mu = & + g^* \left[\begin{pmatrix} Y_1^2 + Y_2^2 & 0 & 0 \\ 0 & 0 & Y_1^2 + Y_2^2 \\ 0 & Y_1^2 + Y_2^2 & 0 \end{pmatrix}^* \right. \\ & + r_{g1} e^{-ip_{g1}} \begin{pmatrix} Y_2^2 - Y_1^2 & 0 & 0 \\ 0 & \sqrt{3}Y_1 Y_2 & -\frac{1}{2}(Y_2^2 - Y_1^2) \\ 0 & -\frac{1}{2}(Y_2^2 - Y_1^2) & \sqrt{3}Y_1 Y_2 \end{pmatrix}^* \\ & \left. + r_{g2} e^{-ip_{g2}} \begin{pmatrix} 0 & -(\sqrt{3}Y_1 Y_5 + Y_2 Y_4) & \sqrt{3}Y_1 Y_4 + Y_2 Y_4 \\ -(\sqrt{3}Y_1 Y_5 + Y_2 Y_4) & 2Y_2 Y_3 & 0 \\ \sqrt{3}Y_1 Y_4 + Y_2 Y_4 & 0 & -2Y_2 Y_3 \end{pmatrix}^* \right]. \quad (16) \end{aligned}$$

The singlet-right-handed neutrino coupling reads

$$\mathbf{B1} : M_S = \Lambda^* \begin{pmatrix} 0 & -Y_3 \\ \frac{\sqrt{3}}{2}Y_4 & \frac{1}{2}Y_5 \\ \frac{\sqrt{3}}{2}Y_5 & \frac{1}{2}Y_4 \end{pmatrix}^* , \quad (17)$$

$$\begin{aligned} \mathbf{B2} : M_S = & + \Lambda^* \left[\begin{pmatrix} -2Y_2Y_3 & 0 \\ -\frac{1}{2}(\sqrt{3}Y_1Y_4 + Y_2Y_5) & \frac{\sqrt{3}}{2}(\sqrt{3}Y_1Y_5 + Y_2Y_4) \\ -\frac{1}{2}(\sqrt{3}Y_1Y_5 + Y_2Y_4) & \frac{\sqrt{3}}{2}(\sqrt{3}Y_1Y_4 + Y_2Y_5) \end{pmatrix}^* \right. \\ & \left. + r_\Lambda e^{-ip_\Lambda} \begin{pmatrix} 0 & -2Y_1Y_3 \\ \frac{\sqrt{3}}{2}(\sqrt{3}Y_2Y_5 - Y_1Y_4) & \frac{1}{2}(\sqrt{3}Y_2Y_4 - Y_1Y_5) \\ \frac{\sqrt{3}}{2}(\sqrt{3}Y_2Y_4 - Y_1Y_5) & \frac{1}{2}(\sqrt{3}Y_2Y_5 - Y_1Y_4) \end{pmatrix}^* \right] . \end{aligned} \quad (18)$$

The Dirac neutrino mass term is

$$\mathbf{C1} : M_D = y^* v_u \begin{pmatrix} 0 & -Y_3 \\ \frac{\sqrt{3}}{2}Y_4 & \frac{1}{2}Y_5 \\ \frac{\sqrt{3}}{2}Y_5 & \frac{1}{2}Y_4 \end{pmatrix}^* , \quad (19)$$

$$\begin{aligned} \mathbf{C2} : M_D = & + y^* v_u \left[\begin{pmatrix} -2Y_2Y_3 & 0 \\ -\frac{1}{2}(\sqrt{3}Y_1Y_4 + Y_2Y_5) & \frac{\sqrt{3}}{2}(\sqrt{3}Y_1Y_5 + Y_2Y_4) \\ -\frac{1}{2}(\sqrt{3}Y_1Y_5 + Y_2Y_4) & \frac{\sqrt{3}}{2}(\sqrt{3}Y_1Y_4 + Y_2Y_5) \end{pmatrix}^* \right. \\ & \left. + r_y v_u e^{-ip_y} \begin{pmatrix} 0 & -2Y_1Y_3 \\ \frac{\sqrt{3}}{2}(\sqrt{3}Y_2Y_5 - Y_1Y_4) & \frac{1}{2}(\sqrt{3}Y_2Y_4 - Y_1Y_5) \\ \frac{\sqrt{3}}{2}(\sqrt{3}Y_2Y_4 - Y_1Y_5) & \frac{1}{2}(\sqrt{3}Y_2Y_5 - Y_1Y_4) \end{pmatrix}^* \right] , \end{aligned} \quad (20)$$

where $v_u \equiv \langle H_u \rangle$ is the vev of the up-type Higgs doublet.

The 8×8 mass matrix written in the basis (ν_L, N_R^C, S_L) is

$$\mathcal{M} = \begin{pmatrix} \mathbf{0}_{3 \times 3} & [M_D]_{3 \times 2} & \mathbf{0}_{3 \times 3} \\ [M_D^T]_{2 \times 3} & \mathbf{0}_{2 \times 2} & [M_S^T]_{2 \times 3} \\ \mathbf{0}_{3 \times 3} & [M_S]_{3 \times 2} & [\mu]_{3 \times 3} \end{pmatrix} . \quad (21)$$

After block diagonalization, one gets the light neutrino mass matrix as

$$M_\nu = -M_D (M_S^T M_S)^{-1} M_S^T \mu M_S (M_S^T M_S)^{-1} M_D^T . \quad (22)$$

The M_ν expression looks slightly different from that in the canonical ISS case (see Appendix C), mainly due to the complexity caused by the rectangular shape of M_D and M_S matrices. By the canonical ISS model we mean models with $n_{N_R} = n_{S_L}$, where n_{N_R} and n_{S_L} stand for the number

of N_R and that of S_L respectively. Details of the block diagonalization procedure can be found in Appendix C.

The light neutrino mass matrix can be diagonalized by a unitary matrix U as $U^\dagger M_\nu U^* = \widehat{M}_\nu$, where $\widehat{M}_\nu \equiv \text{Diag}\{m_1, m_2, m_3\}$ with m_i being neutrino masses. The neutrino flavor mixing matrix is non-unitary (but we still use the symbol U_ν) and connected to the unitary one U as

$$U_\nu = (1 - \eta)U, \quad (23)$$

where the η matrix measures the unitarity violation and is approximately given by $\eta \simeq RR^\dagger/2$. The R matrix comes from the block diagonalization and can be expressed as

$$R = \left[M_D^* \left(M_S^\dagger M_S^* M_S^\dagger M_S^* \right)^{-1} M_S^\dagger \mu^* M_S^* - M_D^* \left(M_S^\dagger M_S^* \right)^{-1} M_S^\dagger \right]_{3 \times 5}, \quad (24)$$

which leads to $\eta \simeq M_D^* \left(M_S^\dagger M_S^* \right)^{-1} M_D^T/2$, where the higher-order term $\mathcal{O}(\mu^2 M_D^2/M_S^4)$ has been omitted. From Eq. (22) we see that the light neutrino mass is at $\mathcal{O}(\mu M_D^2/M_S^2)$. Considering a hierarchy $\mu \ll M_D < M_S$, e.g., $\mu \sim 1$ keV, $M_D \sim 10^2$ GeV, $M_S \sim 10^4$ GeV, one can have sub-eV masses for light neutrinos.

3 Lepton Flavor Mixing

As neutrino oscillation parameters are precisely measured, we first consider the constraints on the models from neutrino oscillation. To make a comparison with the observables, we take the leading-order approximation, i.e., taking the effective Majorana neutrino mass matrix in Eq. (22) and the charged lepton mass matrix in Eq. (13) as the starting point. By diagonalizing both, we get observables as functions of model parameters. As pointed out in the last section, in ISS models, the light neutrino mixing matrix is not unitary. However, the non-unitarity is stringently constrained by current experiments. Ref. [37] offers a global fit of constraints on leptonic unitarity, from which one can see that, even in the agnostic case,² the row and column normalizations agree well with one, i.e., the unitary value. The 3σ credible regions (CR) allow only percent-level deviations from one in the first and second row and a few tens percent of the rest. It is reasonable to assume the unitarity at the leading order.

We perform a Bayesian model comparison among the twenty-four candidate scenarios (twelve models with both mass orderings of the light neutrinos). We construct a seven-dimensional Gaussian likelihood function using observables from Table 2. The number of model parameters is counted as follows: 2 real parameters from the modulus τ , plus 3 parameters in the charged lepton sector, plus N parameters in the neutrino sector, where N is model-dependent and is listed in the following:

$$\begin{aligned} \mathbf{A1}, \mathbf{A2} : & 0 \\ \mathbf{A3} : & 4 (r_{g1}, r_{g2}, p_{g1}, p_{g2}) \\ \mathbf{B1}, \mathbf{C1} : & 0 \\ \mathbf{B2}, \mathbf{C2} : & 2 (r_\Lambda, p_\Lambda \text{ or } r_y, p_y) \end{aligned}$$

²The agnostic case refers to the matrix \mathcal{U} defined in $\nu_\alpha = \sum_k \mathcal{U}_{\alpha k} \nu_k$ is not unitary. Here $\alpha \in e, \mu, \tau, \dots$ is the flavor index, $k \in 1, 2, 3, \dots$ is the index for mass eigenstates. The agnostic case has the largest non-unitarity effects. ISS models correspond to a submatrix case where the matrix \mathcal{U} is unitary. The non-unitarity in the submatrix case is a subset of that in the agnostic case, as shown in Fig. 13 of Ref. [37].

Table 2: The observables in the charged lepton and neutrino sector. The charged lepton Yukawa couplings are evaluated at the m_Z scale, taken from Ref. [41]. The neutrino oscillation parameters are taken from NuFIT 5.0 (2020) [42]. The average errors are shown in the brackets.

y_e	$2.7771(26) \times 10^{-6}$	
y_μ	$5.8504(13) \times 10^{-4}$	
y_τ	$9.9372(16) \times 10^{-3}$	
	NO	IO
$\sin^2 \theta_{12}$	0.304(13)	0.304(13)
$\sin^2 \theta_{13}$	0.02221(65)	0.02240(62)
$\sin^2 \theta_{23}$	0.570(21)	0.575(19)
$r \equiv \frac{\Delta m_{21}^2}{ \Delta m_{31(2)}^2 }$	0.0295(9)	0.0297(9)

Table 3: The best-fit values of the model parameters.

$\text{Re}\tau$	$\text{Im}\tau$	α	β	γ	r_Λ	r_y	p_Λ	p_y
0.260	1.762	7.110×10^{-4}	1.719×10^{-2}	2.999×10^{-6}	0.847	0.312	3.913	2.370

Table 4: The observables calculated from the best-fit parameters and the predictions for the phases.

Parameters	Predicted value
$\sin^2 \theta_{12}$	0.305
$\sin^2 \theta_{13}$	0.02227
$\sin^2 \theta_{23}$	0.571
$\frac{\Delta m_{21}^2}{\Delta m_{31}^2}$	0.0296
y_e	2.7774×10^{-6}
y_μ	5.8505×10^{-4}
y_τ	9.9372×10^{-3}
δ [$^\circ$]	108.9
α_{21} [$^\circ$]	25.8
α_{31} [$^\circ$]	52.7

With noncommittal model priors, the model selection is made by comparing the Bayesian factors. We use MultiNest [38–40] to sample and evaluate the Bayesian evidence. The priors are set on the same rooting to avoid any bias on evidence evaluation. We find that among the 24 candidate scenarios, there is strong preference for normal ordering of **A1B2C2**. In the following, we explore the parameter space of model **A1B2C2** in detail to see if it can be in accordance with the oscillation data.

Running MultiNest in a parameter-estimation mode, we find the best-fit values of parameters

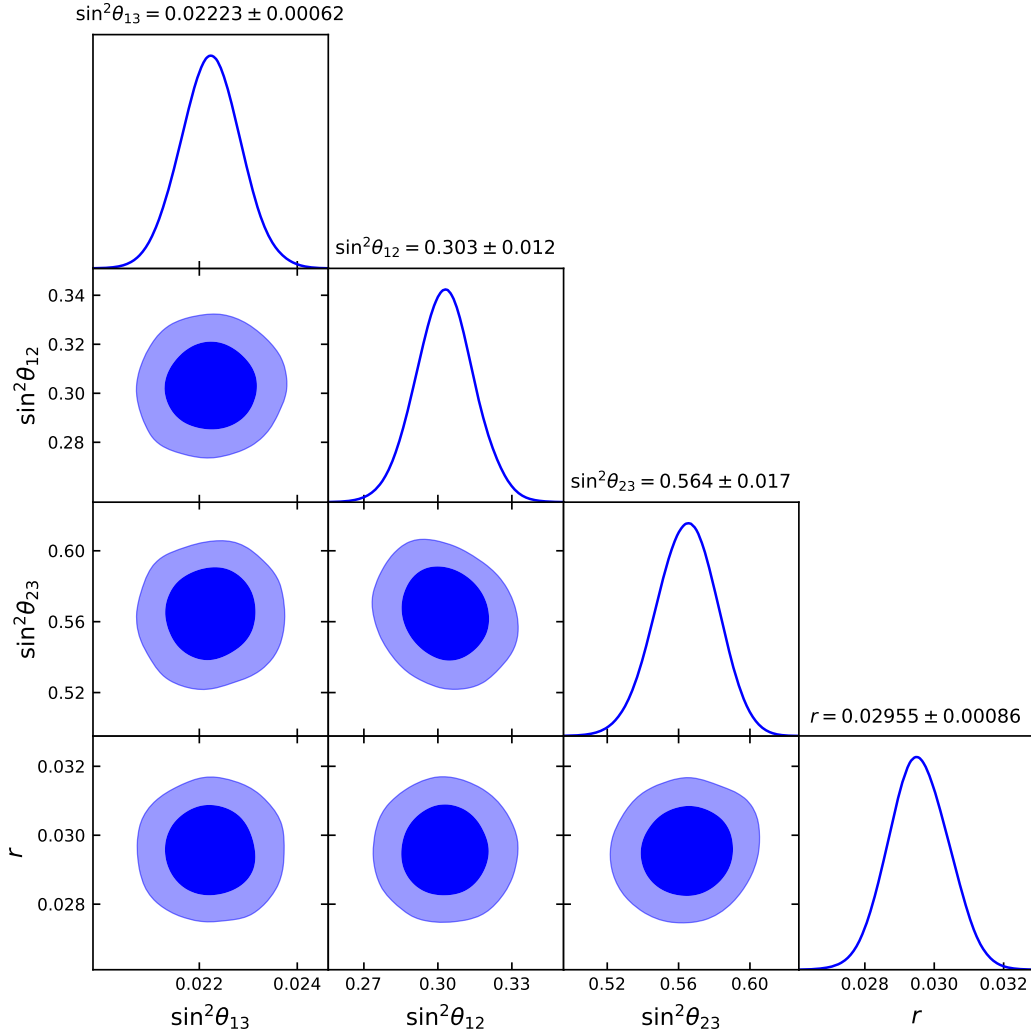


Figure 1: The one- and two-dimensional posterior distribution of the model **A1B2C2** observables in the neutrino sector. The light and dark blue region correspond to 68% and 95% CR. We also show the mean values with 1σ error. The plot is generated using GetDist [43].

(shown in Table 3) correspond to $\chi^2_{\min} \simeq 0.04$, which shows a remarkable agreement with experimental observations. The values of the observables and predictions for the phases corresponding to the best-fit parameters are given in Table 4. We also show the one- and two-dimensional posterior distributions of the model observables in the neutrino sector in Fig. 1. From these results, we see an excellent agreement with the constraining observables. At this stage, the lepton mixing is totally solved. The predicted value for the Dirac CP-violating phase is within 3σ range. We also have predictions on the two Majorana CP-violating phases defined as follows

$$U = \begin{pmatrix} c_{12}c_{13} & s_{12}c_{13} & s_{13}e^{-i\delta} \\ -s_{12}c_{23} - c_{12}s_{23}s_{13}e^{i\delta} & c_{12}c_{23} - s_{12}s_{23}s_{13}e^{i\delta} & s_{23}c_{13} \\ s_{12}s_{23} - c_{12}c_{23}s_{13}e^{i\delta} & -c_{12}s_{23} - s_{12}c_{23}s_{13}e^{i\delta} & c_{23}c_{13} \end{pmatrix} \begin{pmatrix} 1 & 0 & 0 \\ 0 & e^{i\alpha_{21}/2} & 0 \\ 0 & 0 & e^{i\alpha_{31}/2} \end{pmatrix}. \quad (25)$$

The predicted 3σ CR are

$$\delta \in [69.3, 139.8]^\circ, \quad \alpha_{21} \in [-18.9, 108.3]^\circ, \quad \alpha_{31} \in [-53.9, 123.2]^\circ, \quad (26)$$

and the best-fit values are shown in Table 4.

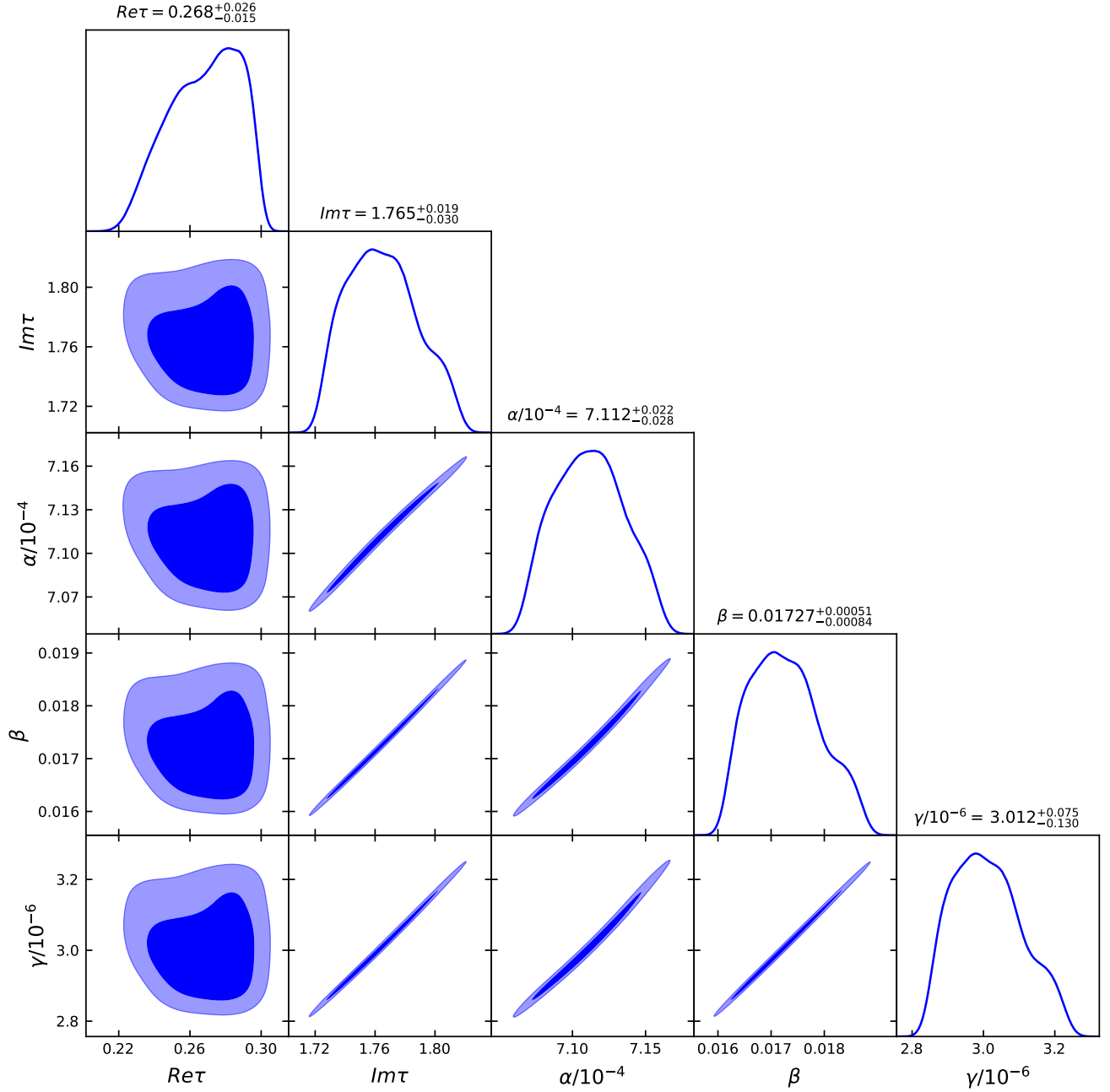


Figure 2: The one- and two-dimensional posterior distribution of the model **A1B2C2** parameters. The light and dark blue region correspond to 68% and 95% CR. We also show the mean parameter values with 1σ error. The plot is generated using GetDist [43].

Although the number of model parameters is larger than that of the observables, it is not a trivial fit as the actual number of degrees of freedom is small. As can be seen from the two-dimensional posterior distribution of the model parameter in Fig. 2, the parameters α , β , γ are strongly correlated with $\text{Im}\tau$, reducing the effective number of degrees of freedom to six.

The strong correlation of the parameters can be understood using analytical approximation, which is applicable given that the best-fit value of $\text{Im}\tau$ is large. We introduce

$$x \equiv \exp(-\pi \text{Im}\tau/2), \quad y \equiv \pi \text{Re}\tau/2,$$

such that $q^{1/4} = xe^{iy}$. Given the best-fit value $\text{Im}\tau = 1.762$, we find that $x \simeq 0.063$ can be a good perturbative parameter. Expanding the basis in x , at the leading order, we get

$$Y_1 \simeq -3\pi/8 ; \quad (27)$$

$$Y_2 \simeq 3\sqrt{3}\pi x^2 e^{2iy} ; \quad (28)$$

$$Y_3 \simeq \pi/4 ; \quad (29)$$

$$Y_4 \simeq -\sqrt{2}\pi x e^{iy} ; \quad (30)$$

$$Y_5 \simeq -4\sqrt{2}\pi x^3 e^{3iy} . \quad (31)$$

The charged lepton mass matrix at the leading order reads

$$M_l \simeq v_d \begin{pmatrix} \frac{1}{4}\pi\alpha & 0 & -\frac{3}{16}\pi^2\gamma \\ 0 & 0 & 0 \\ 0 & 0 & 0 \end{pmatrix} + v_d x e^{-iy} \begin{pmatrix} 0 & 0 & 0 \\ 0 & \frac{3}{4}\sqrt{\frac{3}{2}}\pi^2\beta & 0 \\ -\sqrt{2}\pi\alpha & 0 & -\frac{3}{4\sqrt{2}}\pi^2\gamma \end{pmatrix} . \quad (32)$$

To find U_l , it is convenient to use

$$M_l M_l^\dagger \simeq v_d^2 \begin{pmatrix} \frac{\pi^2}{256}(16\alpha^2 + 9\pi^2\gamma^2) & 0 & \frac{\pi^2}{64\sqrt{2}}(-32\alpha^2 + 9\pi^2\gamma^2)x e^{iy} \\ 0 & \frac{27}{32}\pi^4\beta^2 x^2 & 0 \\ \frac{\pi^2}{64\sqrt{2}}(-32\alpha^2 + 9\pi^2\gamma^2)x e^{-iy} & 0 & \frac{\pi^2}{32}(64\alpha^2 + 9\pi^2\gamma^2)x^2 \end{pmatrix} , \quad (33)$$

where we neglect higher-order terms $\mathcal{O}(x^4)$. One can see that the charged lepton sector contributes a 1-3 rotation up to $\mathcal{O}(x^2)$. To fit the charged lepton Yukawas, x or $\text{Im}\tau$ is strongly correlated with α , β , γ , as can be seen from the eigenvalues of $M_l M_l^\dagger$, i.e.,

$$y_e^2 \simeq \frac{81\pi^4\alpha^2\gamma^2 x^2}{32\alpha^2 + 18\pi^2\gamma^2} ; \quad (34)$$

$$y_\mu^2 \simeq \frac{27}{32}\pi^4\beta^2 x^2 ; \quad (35)$$

$$y_\tau^2 \simeq \frac{1}{256}\pi^2 (16\alpha^2 + 9\pi^2\gamma^2) + \frac{(32\pi\alpha^2 - 9\pi^3\gamma^2)^2 x^2}{32(16\alpha^2 + 9\pi^2\gamma^2)} , \quad (36)$$

where the higher-order contributions are neglected. Taking the leading contribution and using the best-fit value of x allow a rough estimation of $\alpha \sim \mathcal{O}(10^{-2})$, $\beta \sim \mathcal{O}(10^{-3})$, $\gamma \sim \mathcal{O}(10^{-6})$. These magnitudes roughly agree with those we get from the best fit. The point is that x , together with the three coefficients α , β , γ , are fixed by the charged lepton mass spectrum, so they are correlated as shown in Fig. 2.

To estimate the magnitude of the 1-3 rotation, we introduce $H \equiv M_l M_l^\dagger$, and use the fact that $U_l^\dagger H U_l = \text{Diag}\{m_e^2, m_\mu^2, m_\tau^2\}$, where U_l is parameterized in the standard way with only a nonzero rotation angle θ_{13}^l . We have

$$H_{11} = \frac{1}{2} [m_e^2 + m_\tau^2 - (m_\tau^2 - m_e^2) \cos 2\theta_{13}^l] ; \quad (37)$$

$$H_{33} = \frac{1}{2} [m_e^2 + m_\tau^2 + (m_\tau^2 - m_e^2) \cos 2\theta_{13}^l] ; \quad (38)$$

$$|H_{13}| = |H_{31}| = \frac{1}{2} (m_\tau^2 - m_e^2) \sin 2\theta_{13}^l . \quad (39)$$

Looking back at Eq. (33), we find

$$\tan 2\theta_{13}^l = \frac{2|H_{13}|}{H_{33} - H_{11}} \simeq 8\sqrt{2}x, \quad (40)$$

which renders $\theta_{13}^l \simeq 18^\circ$ with the best-fit value of x . This value is comparable to the one get from the best fit, i.e., 10° .

The light neutrino mass matrix reads

$$\begin{aligned} M_\nu \simeq & - \begin{pmatrix} \frac{r_y^2}{r_\Lambda^2} & 0 & 0 \\ 0 & 0 & 0 \\ 0 & 0 & 0 \end{pmatrix} \\ & + x e^{-2iy} \frac{\sqrt{2}r_y}{r_\Lambda^2} \begin{pmatrix} 0 & * & * \\ \frac{(r_\Lambda - 3e^{ip_\Lambda})(r_y + e^{ip_y})}{r_\Lambda + e^{ip_\Lambda}} & 0 & 0 \\ r_y - 3e^{ip_y} & 0 & 0 \end{pmatrix} \\ & - x^2 e^{-2iy} \frac{2}{r_\Lambda^2} \begin{pmatrix} \frac{2(r_\Lambda - 3e^{ip_\Lambda})^2 r_y^2}{r_\Lambda^2} & 0 & 0 \\ 0 & 0 & * \\ 0 & \frac{(r_\Lambda - 3e^{ip_\Lambda})(r_y - 3e^{ip_\Lambda})(r_y + e^{ip_y})}{r_\Lambda + e^{ip_\Lambda}} & (r_y - 3e^{ip_y})^2 \end{pmatrix}, \end{aligned} \quad (41)$$

where “*” denotes the symmetric counterpart, we neglect the overall unphysical phase $e^{2i(p_\Lambda - p_y)}$, and we omit the higher-order terms starting from $\mathcal{O}(x^3)$. With the help of the best-fit values of parameters, we find the non-vanishing entities in M_ν up to $\mathcal{O}(x^2)$ are all of the same magnitude, which makes it difficult to proceed with the analytical approximation. It takes three relatively large rotations to be transformed into diagonal, which is verified by the best-fit parameter values. We observe that the (μ, μ) entity in M_ν is vanishing. As it is a function of all the mixing angles and phases, among which two Majorana phases are completely unknown, and the Dirac phase is loosely constrained, it is hard to draw any conclusion from this condition.

Note that by far, the full neutrino mass spectrum is not shown, which is only available when we specify the scales of each sector, namely, the coefficients of the matrices M_D , M_S , μ . With these values, we can solve the full neutrino mass matrix in Eq. (21) and determine the active-sterile neutrino mixing. This analysis is performed in the next section, and we provide the conclusion here: the absolute light neutrino mass scale in this model is $m_{\min} \in [10^{-4}, 0.1]$ eV, by constraints from both lepton flavor mixing and the keV sterile neutrino dark matter. A large portion of this range is within the aggressive combined (oscillation + non-oscillation) constraint, and nearly all this range is allowed by the conservative combined constraint [44].

4 keV Sterile Neutrino

4.1 Warm Dark Matter

In this subsection, we briefly review the basics of keV-mass sterile neutrinos as a candidate for warm dark matter (WDM). We start with an introduction to the stability and mass scale, and to possible production mechanisms, and then discuss observational constraints from astrophysical X-ray search and Lyman- α forest data.

4.1.1 Stability and Mass Scale

The basic requirements for a particle dark matter candidate are electrically neutral and stable. Mixing with light active neutrinos, the sterile state is not absolutely stable. It can decay into a light active neutrino and a photon, or three neutrinos. Its lifetime is estimated from the inverse of the total decay rate, which is found to be larger than the age of the Universe as long as the mixing with active neutrinos is small.

Being a fermion dark matter candidate, in our case a sterile neutrino, its mass gets a lower bound by requiring that the maximal kinetic energy it can have is no larger than the gravitational potential energy, i.e., it is gravitationally bounded. From the observed dwarf satellite galaxy mass and radius, one gets the Tremaine-Gunn bound [45],

$$m_s \gtrsim 0.5 \text{ keV} . \quad (42)$$

This is the first argument that sets the sterile neutrino dark matter mass to be keV.

It is a generic feature of ISS models that when $n_{S_L} > n_{N_R}$ there will be $(n_{S_L} - n_{N_R})$ intermediate-mass states at the scale μ [17]. Actually, the whole mass spectrum for neutrinos including the steriles is

- n_{ν_L} light active neutrinos $\mathcal{O}(\mu M_D^2/M_S^2)$
- $(n_{S_L} - n_{N_R})$ light sterile states $\mathcal{O}(\mu)$
- $2n_{N_R}$ heavy states $\mathcal{O}(M_S)$, which form n_{N_R} pseudo-Dirac pairs

Given $\mu \sim 1 \text{ keV}$, $M_D \sim 10^2 \text{ GeV}$ and $M_S \sim 10^4 \text{ GeV}$, we expect a sterile neutrino at the keV scale. The detailed numerical analysis of the mass spectrum will be given in next subsection.

4.1.2 Production Mechanism

In general, keV sterile neutrinos can be produced in the following ways:

- Dodelson-Widrow (DW) mechanism [46], in which the sterile neutrino is produced through active-sterile transition at $T \sim 100 \text{ MeV}$ in the primordial plasma, which is always allowed as long as the active-sterile mixing exists.
- Shi-Fuller (SF) mechanism [47], in which a pre-existing lepton number asymmetry produces an enhancement of the active-sterile neutrino transition rate, which is in close analog with the Mikheyev-Smirnov-Wolfenstein matter effect [48–50] and is also known as the resonant production mechanism.

As the sterile neutrinos can only interact feebly (by definition), they cannot be produced in thermal equilibrium. Both of the aforementioned production mechanisms produce a non-thermal momentum distribution. While the DW mechanism gives rise to the thermal distribution with a suppression factor, the SF mechanism usually leads to a “colder” distribution. There exist other mechanisms for keV sterile neutrino production (see Refs. [51–55] for a general introduction), which require either extra particles or extended gauge symmetries, thus are not applicable to our case.

4.1.3 Constraints from Astrophysics and Structure Formation

To be a viable dark matter candidate, keV sterile neutrinos have to survive several observational constraints. The first one is the dark matter abundance observed today, which is $\Omega_{\text{DM}} = 0.120 \pm 0.001$ given by Planck [56]. The dark matter abundance imposes limits on both dark matter mass and active-sterile mixing, since the dark matter should not be overproduced to overclose the Universe. It is estimated as [57]

$$\Omega_{\text{DM}} h^2 = 1.1 \times 10^7 \sum_{\alpha} C_{\alpha}(m_s) |U_{\alpha s}|^2 \left(\frac{m_s}{\text{keV}} \right)^2, \quad \alpha = e, \mu, \tau, \quad (43)$$

where C_{α} are flavor-dependent coefficients whose exact values can be obtained by solving the Boltzmann equations. It is also possible that sterile neutrinos only serve as a fraction of the total dark matter. In this case, one can introduce an abundance fraction $f_s = \Omega_s / \Omega_{\text{DM}}$, and Ω_{DM} in Eq. (43) should be replaced by $f_s \Omega_{\text{DM}}$.

Given the mixing with active neutrinos, the sterile neutrinos undergo radiative decays $N \rightarrow \nu \gamma$, which produces a mono-chromatic photon with energy $E_{\gamma} \simeq m_s/2$. Such an X -ray line has been searched by Chandra [58], XMM-Newton [59] and NuSTAR [60]. The non-observation of the X -ray puts stringent limits on sterile neutrino mass and mixing.

Being relatively light, sterile neutrinos feature a relatively large free-streaming horizon, which suppresses the small-scale structure of the matter power spectrum, thus get constrained from structure formation. Lyman- α forest data, coming from observing the Lyman- α transition in hydrogen gas of the Universe, gives the intergalactic medium distribution, from which the WDM velocity dispersion can be extracted. Current Lyman- α bound at the 95% confidence level on the WDM mass is [61–65]

$$m_{\text{WDM}} \gtrsim (1.9 - 5.3) \text{ keV}. \quad (44)$$

There are other constraints, e.g., Milky Way satellite galaxies counting [66] and supernova bounds [67–71]. However, these constraints are not competitive with the X -ray bounds and the Lyman- α constraints, so we do not include them. It is worth mentioning that the astrophysical X -ray constraints are model-independent, while the structure formation constraints in Eq. (44) from Lyman- α forest data only directly apply to WDM with a thermal distribution.

4.2 Numerical Results

We now proceed with a numerical analysis of the parameter space by taking account of the constraints on WDM. We solve the active-sterile mixing from the full matrix \mathcal{M} in Eq. (21). After diagonalization, the whole mass spectrum is given by $\widehat{\mathcal{M}} \equiv \text{Diag}\{m_1, m_2, m_3, m_4, m_5, m_6, m_7, m_8\}$. From the generic feature of the mass spectrum in the ISS models as introduced in Sec. 4.1, we identify that the light sterile mass is $m_s \simeq m_4$, and the heavy states form two pseudo-Dirac pairs with masses $m_5 \simeq m_6$ and $m_7 \simeq m_8$. To solve for the mixing and the mass spectrum, we need to restore two coefficient ratios from the three matrices: M_{D} , M_{S} , μ . To show it in a more explicit way, we examine all the three coefficients and set

$$\Lambda = 10^2 \text{ GeV}, \quad yv_{\text{u}} \in [10^{-6}, 10^{-2}] \Lambda, \quad g \in [10^{-4}, 10^{-2}] yv_{\text{u}}. \quad (45)$$

Note that these coefficients do not affect oscillation phenomenology, as long as they fulfill the requirement that the approximation made in Eq. (22) is valid, i.e., $g \ll yv_{\text{u}} \Lambda$. As $(yv_{\text{u}}/\Lambda)^2$ characterizes the magnitude of the non-unitary effect, we require it less than $\mathcal{O}(10^{-4})$ to be in

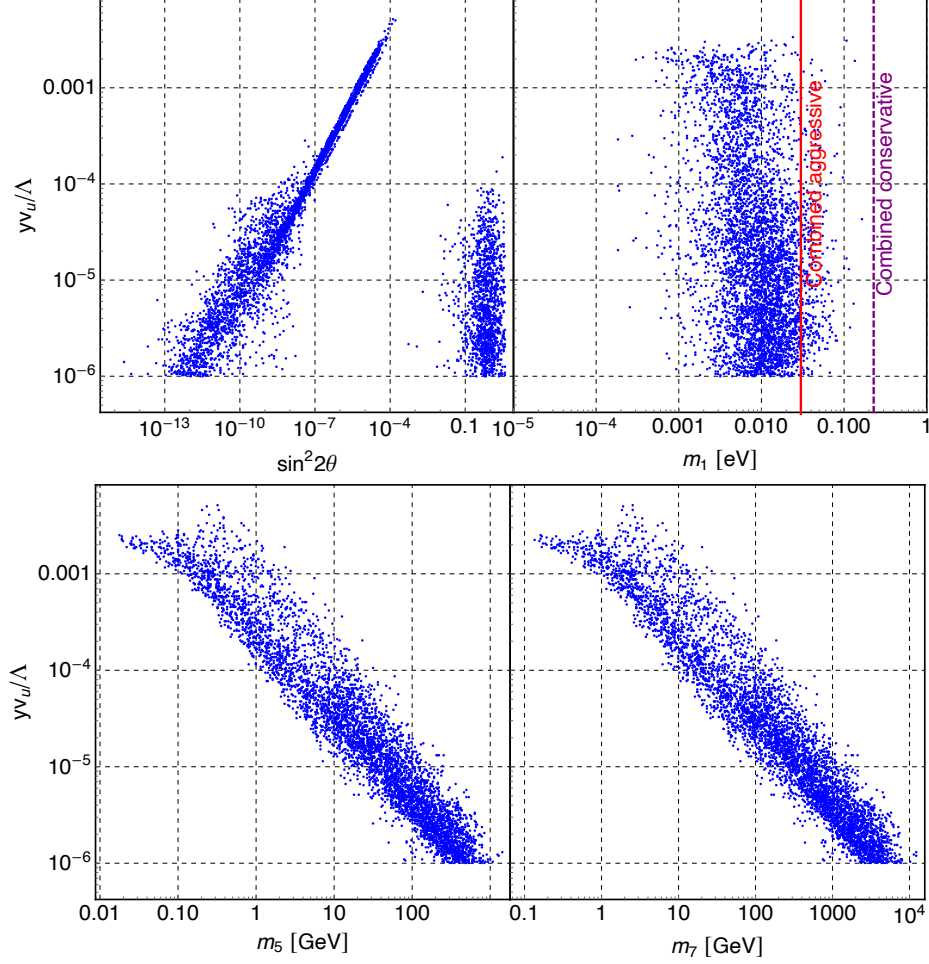


Figure 3: The correlation of the scale ratio yv_u/Λ with the active-sterile mixing, the lightest neutrino mass, and the two heavier sterile neutrino masses. The points are selected from the scan with the light sterile mass $m_s \in [0.5, 50]$ keV. In the upper-right plot, we show the aggressive (red line) and conservative (purple dashed line) combined (oscillation + non-oscillation) constraints from Ref. [44].

no conflict with existing experimental constraints. The value of Λ is chosen only for illustrative purpose. The overall scale is set by the ratio of the neutrino mass-squared differences.

It can be inferred from Eq. (45) that the heavy-state masses can span a large range in the model. It is understandable since the inverse seesaw formula only requires $M_D/M_S \sim \mathcal{O}(10^{-2})$ even if we fix μ at keV. From a numerical scan, we select points with $m_s \in [0.5, 50]$ keV as the viable ones. For the viable points, we find $m_5 \simeq m_6$ and $m_7 \simeq m_8$ as expected. We plot the correlations of the active-sterile mixing, the lightest neutrino mass, two heavy-state masses with the scale ratio yv_u/Λ in Fig. 3. The ratio $g/(yv_u)$ is insensitive to these quantities; thus, we do not show them here.

The constraints from the relic abundance, X-ray search, and the Tremaine-Gunn bound are shown in Fig. 4. From Fig. 4 we see that given the light sterile mass in the desired region, the active-sterile mixing can span a wide range. Although a large range has been excluded either by overabundance or X-ray search, there are still vast surviving points corresponding to an active-sterile mixing $\sin^2 2\theta$ from 10^{-14} to 10^{-7} , depending on the sterile neutrino mass. From the upper-left plot in Fig. 3, we see that this active-sterile mixing window requires yv_u/Λ to be smaller than 10^{-4} . As yv_u/Λ characterizes M_D/M_S , and the non-unitary effect is measured by M_D^2/M_S^2 , we

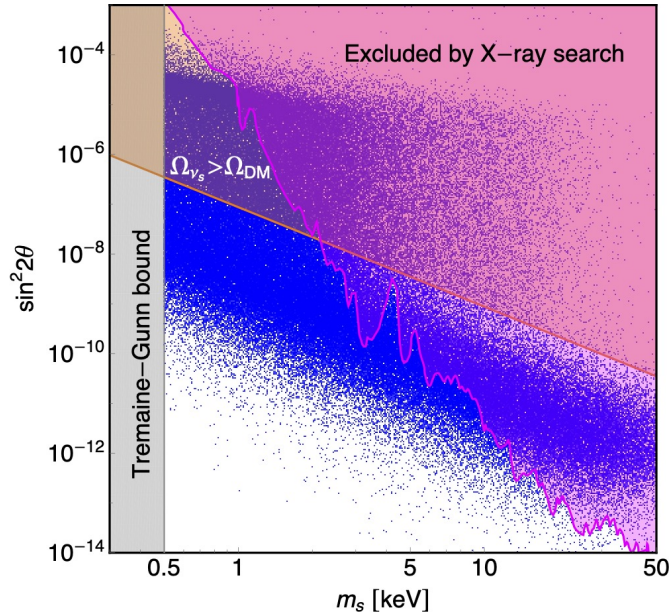


Figure 4: The allowed parameter space shown in the $(m_s, \sin^2 2\theta)$ plane. The light orange area is excluded by the overabundance of dark matter, while the pink area by the non-observation of the X-ray line, where the low-mass region is set mainly by Chandra [58] and XMM-Newton [59], and the high-mass region by NuSTAR [60]. The Tremaine-Gunn bound [45] is also shown.

conclude that the non-unitary effect is vanishingly small. Applying the same argument, we find

$$m_5 \simeq m_6 \in [1, 10^3] \text{ GeV}, \quad m_7 \simeq m_8 \in [10, 10^4] \text{ GeV}. \quad (46)$$

Given the above heavy state masses, one may expect their signatures at the high-energy hadron colliders. A detailed analysis will be carried out elsewhere. The relevant existing studies can be found in Refs. [72–77].

By far we have not put the Lyman- α forest constraints for the reason that it is model-dependent as mentioned in Sec. 4.1. The Lyman- α bounds on m_{WDM} is derived by assuming a Fermi-Dirac distribution for WDM, which is neither the case for DW production nor the case for SF production. Light sterile neutrinos from DW production feature a momentum distribution that can be approximated by a rescaled Fermi-Dirac distribution, and also have nearly the same transfer function as the thermal relics. Therefore, the rescaling relation between m_{WDM} and m_s is valid [62, 78]

$$\frac{m_s}{3.9 \text{ keV}} = \left(\frac{m_{\text{WDM}}}{\text{keV}} \right)^{1.294} \left(\frac{0.25 \times 0.7^2}{\Omega_{\text{DM}} h^2} \right)^{1/3}. \quad (47)$$

This rescaling is only approximate as the momentum distribution from the DW production mechanism differs from a rescaled Fermi-Dirac distribution. Applying the current Lyman- α bound on WDM in Eq. (44), we get a lower bound on light sterile mass as

$$m_s \gtrsim (8.9 - 33.8) \text{ keV}. \quad (48)$$

This lower bound clearly contradicts the X-ray bound, which limits the light sterile neutrino mass to be below 4 keV.³ This combined result shows that DW-produced sterile neutrinos cannot be

³It differs a little from direct observation of Fig. 4, as the dark matter abundance line is drawn with an approximation that all the flavor-dependent coefficients are equal to 0.5.

100% dark matter. This, however, does not rule out the sterile neutrino in this model as a viable dark matter candidate. In what follows, we present a few possible options.

First, if sterile neutrinos produced from the DW mechanism only contribute a fraction of total dark matter, the Lyman- α bounds can be relaxed, thus opening up viable parameter space. Second, heavy states may have an impact as entropy dilution if they once dominate the energy density of the Universe. The inclusion of such an effect can also enlarge viable parameter space, as discussed in Refs. [57, 79, 80]. Third, for SF production, the probability of active-sterile transition gets an enhancement when a lepton asymmetry dominates over the background potential and satisfies the resonant condition. The resulting momentum distribution is “colder” than that of the DW mechanism, thus relaxes the constraints from the small-scale structure. As the momentum distribution is highly non-thermal, no mass-rescaling relation with the WDM can be derived. Hydrodynamical simulations in this case find that sterile neutrinos lighter than 7 keV are inconsistent with the BOSS Lyman- α data [81]. On the other hand, the resonance allows a small mixing for the sterile neutrino production, thus relaxes the X -ray bounds.

5 Conclusion

We construct simple models of neutrino masses and flavor mixing using the modular S_4 as the flavor symmetry group. By introducing two right-handed neutrinos and three singlet fermions, we obtain light neutrino masses through the inverse seesaw mechanism, and we can have an intermediate-scale sterile neutrino which serves as a dark matter candidate. We maintain a minimal field content and utilize all the five irreducible representations in S_4 in a natural way. By requiring that the modular forms having weights no larger than four and taking both light neutrino mass orderings into consideration, we consider twenty-four scenarios.

We perform a Bayesian model selection and find strong preference for the model **A1B2C2** with normal ordering. A detailed analysis shows that the model is in excellent agreement with observations from both the charged lepton and the neutrino sector. There are strong correlations of the model parameters, which reduce the effective degrees of freedom to six. The parameter correlation is explained in an analytical way. With nine model parameters, we get information about all the observables in both charged lepton and neutrino sector, i.e., three charged lepton masses, three light neutrino masses, three mixing angles, and three phases in the lepton mixing matrix, as well as the sterile neutrino spectrum and their mixing with the active neutrinos. From this viewpoint, the model is highly predictive and testable.

With a complete numerical analysis, we find that in the desired sterile neutrino mass range, a large range of the active-sterile mixing is still allowed. Stringent constraints come from the combination of the X -ray search and the Lyman- α forest data. Though being a 100% dark matter generated non-resonantly is ruled out, the sterile neutrino can still be a viable dark matter candidate with one of the following realizations: (i) contribute only a fraction of the total dark matter abundance; (ii) produced with an entropy dilution from the decays of the heavier sterile neutrino states; (iii) produced resonantly.

With an emphasis on the oscillation and dark matter phenomenology, we do not discuss possible collider signatures of the heavy sterile neutrinos. It is an interesting topic and will be studied elsewhere in the future. To sum up, by natural and simple construction, we find one model among all the possibilities in excellent agreement with neutrino masses and mixing and it provides a viable dark matter candidate. The model is highly predictive and can be tested in future oscillation experiments and cosmological observations.

Acknowledgement

This work was supported by the National Natural Science Foundation of China under Grants No. 11775232 and No. 11835013, and by the CAS Center for Excellence in Particle Physics.

Appendices

A Modular Group Theory

The modular group $\bar{\Gamma}$ is the group of linear fractional transformations

$$\tau \rightarrow \gamma\tau = \frac{a\tau + b}{c\tau + d}, \text{ with } a, b, c, d \in \mathbb{Z}, \quad ad - bc = 1, \quad \text{Im}\tau > 0, \quad (49)$$

which act faithfully on the upper-half complex plane. $\bar{\Gamma}$ is isomorphic to the projective special linear group $\text{PSL}(2, \mathbb{Z})$, which is defined as

$$\left\{ \begin{pmatrix} a & b \\ c & d \end{pmatrix} : a, b, c, d \in \mathbb{Z}, \quad ad - bc = 1 \right\} / \{\pm 1\}. \quad (50)$$

The $\text{PSL}(2, \mathbb{Z})$ group has two generators

$$S = \begin{pmatrix} 0 & 1 \\ -1 & 0 \end{pmatrix}, \quad T = \begin{pmatrix} 1 & 1 \\ 0 & 1 \end{pmatrix}. \quad (51)$$

The generators satisfy a minimal set of relation $S^2 = (ST)^3 = I$. Applying S, T to τ , one finds that the two generating transformations for $\bar{\Gamma}$ are

$$\tau \xrightarrow{S} -\frac{1}{\tau}, \quad \tau \xrightarrow{T} \tau + 1. \quad (52)$$

The principal congruence subgroups $\Gamma(N), N = 1, 2, 3, \dots$ are defined as

$$\Gamma(N) = \left\{ \begin{pmatrix} a & b \\ c & d \end{pmatrix} \in \text{SL}(2, \mathbb{Z}), \quad \begin{pmatrix} a & b \\ c & d \end{pmatrix} \equiv \begin{pmatrix} 1 & 0 \\ 0 & 1 \end{pmatrix} \pmod{N} \right\}. \quad (53)$$

$\Gamma(N)$ are infinite normal subgroups of the special linear group $\text{SL}(2, \mathbb{Z}) = \Gamma(1) = \bar{\Gamma}$, which is the group of 2×2 matrices with integer elements and determinant 1. With

$$N = 1, 2, \quad \bar{\Gamma}(N) \equiv \Gamma(N) / \{I, \pm I\}; \quad (54)$$

$$N > 2, \quad \bar{\Gamma}(N) \equiv \Gamma(N), \quad (55)$$

one can introduce the finite modular groups as the quotient groups $\Gamma_N \equiv \bar{\Gamma} / \bar{\Gamma}(N)$. For $N \leq 5$, Γ_N are isomorphic to permutation groups, i.e., $\Gamma_2 \simeq S_3$, $\Gamma_3 \simeq A_4$, $\Gamma_4 \simeq S_4$, and $\Gamma_5 \simeq A_5$.

In modular-invariant supersymmetric theories (SUSY), e.g., $\mathcal{N} = 1$ global SUSY, the action is

$$\mathcal{S} = \int d^4x d^2\theta d^2\bar{\theta} K(\chi_i, \bar{\chi}_i) + \int d^4x d^2\theta W(\chi_i) + \text{h.c.}, \quad (56)$$

where K is the Kähler potential, W is the superpotential and χ_i are the chiral superfields. Requiring the action being invariant under Γ_N leads to the following transformation for the chiral superfields

$$\chi_i \rightarrow (c\tau + d)^{-k_i} \rho_i(\gamma) \chi_i, \quad (57)$$

where ρ_i are the unitary representation matrices and k_i are modular weights carried by superfields χ_i . The invariance of the action requires the superpotential being invariant while the Kähler potential is invariant up to a Kähler transformation,

$$W(\chi_i) \rightarrow W(\chi_i) , \quad (58)$$

$$K(\chi_i, \bar{\chi}_i) \rightarrow K(\chi_i, \bar{\chi}_i) + f(\chi_i) + f(\bar{\chi}_i) . \quad (59)$$

It is more relevant to focus on the superpotential, which can be expressed as

$$W = \sum_n \sum_{\{i_1, \dots, i_n\}} (Y_{\{i_1, \dots, i_n\}}(\tau) \chi_{i_1}, \dots, \chi_{i_n})_{\mathbf{1}} . \quad (60)$$

The invariance of the superpotential requires the coefficient functions $Y(\tau)$ transforming under Γ_N as

$$Y(\tau) \rightarrow Y(\gamma\tau) = (c\tau + d)^{k_Y} \rho_Y(\gamma) Y(\tau) . \quad (61)$$

To make the superpotential invariant, the modular weights and the representations should satisfy

$$k_Y = k_{i_1} + \dots + k_{i_n} , \quad (62)$$

$$\rho_Y \otimes \rho_{I_1} \otimes \dots \supset \mathbf{1} . \quad (63)$$

B Modular Group S_4

The S_4 group is made from permutations of four objects. It has five irreducible representations: $\mathbf{1}, \mathbf{1}', \mathbf{2}, \mathbf{3}$ and $\mathbf{3}'$, and two generators satisfying the following condition:

$$S^2 = T^4 = (ST)^3 = I . \quad (64)$$

Working in a symmetric basis, we collect the expressions of the generators, the Clebsch-Gordan coefficients, the q -expansion of the basis, and the modular-form multiplets of the low weights here for reader's convenience. These results are taken from Ref. [24].

The generators in the five irreducible representations are all symmetric matrices, i.e.,

$$\mathbf{1} : S = 1, \quad T = 1 , \quad (65)$$

$$\mathbf{1}' : S = -1, \quad T = -1 , \quad (66)$$

$$\mathbf{2} : S = \frac{1}{2} \begin{pmatrix} -1 & \sqrt{3} \\ \sqrt{3} & 1 \end{pmatrix} , \quad T = \begin{pmatrix} 1 & 0 \\ 0 & -1 \end{pmatrix} , \quad (67)$$

$$\mathbf{3} : S = -\frac{1}{2} \begin{pmatrix} 0 & \sqrt{2} & \sqrt{2} \\ \sqrt{2} & -1 & 1 \\ \sqrt{2} & 1 & -1 \end{pmatrix} , \quad T = - \begin{pmatrix} 1 & 0 & 0 \\ 0 & i & 0 \\ 0 & 0 & -i \end{pmatrix} , \quad (68)$$

$$\mathbf{3}' : S = \frac{1}{2} \begin{pmatrix} 0 & \sqrt{2} & \sqrt{2} \\ \sqrt{2} & -1 & 1 \\ \sqrt{2} & 1 & -1 \end{pmatrix} , \quad T = \begin{pmatrix} 1 & 0 & 0 \\ 0 & i & 0 \\ 0 & 0 & -i \end{pmatrix} . \quad (69)$$

From the generator matrices, one can derive the Clebsch-Gordan coefficients of tensor products

of two multiplets α and β as follows.

$$\mathbf{1}' \otimes \mathbf{1}' = \mathbf{1}, \quad \mathbf{1} \sim \alpha_1 \beta_1, \quad (70)$$

$$\mathbf{1}' \otimes \mathbf{2} = \mathbf{2}, \quad \mathbf{2} \sim \begin{pmatrix} -\alpha_1 \beta_2 \\ \alpha_1 \beta_1 \end{pmatrix}, \quad (71)$$

$$\mathbf{1}' \otimes \mathbf{3} = \mathbf{3}', \quad \mathbf{3}' \sim \begin{pmatrix} \alpha_1 \beta_1 \\ \alpha_1 \beta_2 \\ \alpha_1 \beta_3 \end{pmatrix}, \quad (72)$$

$$\mathbf{1}' \otimes \mathbf{3}' = \mathbf{3}, \quad \mathbf{3} \sim \begin{pmatrix} \alpha_1 \beta_1 \\ \alpha_1 \beta_2 \\ \alpha_1 \beta_3 \end{pmatrix}, \quad (73)$$

$$\mathbf{2} \otimes \mathbf{2} = \mathbf{1} \oplus \mathbf{1}' \oplus \mathbf{2} \quad (74)$$

$$\mathbf{1} \sim \alpha_1 \beta_1 + \alpha_2 \beta_2, \quad \mathbf{1}' \sim \alpha_1 \beta_2 - \alpha_2 \beta_1, \quad \mathbf{2} \sim \begin{pmatrix} \alpha_2 \beta_2 - \alpha_1 \beta_1 \\ \alpha_1 \beta_2 + \alpha_2 \beta_1 \end{pmatrix},$$

$$\mathbf{2} \otimes \mathbf{3} = \mathbf{3} \oplus \mathbf{3}' \quad (75)$$

$$\mathbf{3} \sim \begin{pmatrix} \alpha_1 \beta_1 \\ \frac{\sqrt{3}}{2} \alpha_2 \beta_3 - \frac{1}{2} \alpha_1 \beta_2 \\ \frac{\sqrt{3}}{2} \alpha_2 \beta_2 - \frac{1}{2} \alpha_1 \beta_3 \end{pmatrix}, \quad \mathbf{3}' \sim \begin{pmatrix} -\alpha_2 \beta_1 \\ \frac{\sqrt{3}}{2} \alpha_1 \beta_3 + \frac{1}{2} \alpha_2 \beta_2 \\ \frac{\sqrt{3}}{2} \alpha_1 \beta_2 + \frac{1}{2} \alpha_2 \beta_3 \end{pmatrix},$$

$$\mathbf{2} \otimes \mathbf{3}' = \mathbf{3} \oplus \mathbf{3}' \quad (76)$$

$$\mathbf{3} \sim \begin{pmatrix} -\alpha_2 \beta_1 \\ \frac{\sqrt{3}}{2} \alpha_1 \beta_3 + \frac{1}{2} \alpha_2 \beta_2 \\ \frac{\sqrt{3}}{2} \alpha_1 \beta_2 + \frac{1}{2} \alpha_2 \beta_3 \end{pmatrix}, \quad \mathbf{3}' \sim \begin{pmatrix} \alpha_1 \beta_1 \\ \frac{\sqrt{3}}{2} \alpha_2 \beta_3 - \frac{1}{2} \alpha_1 \beta_2 \\ \frac{\sqrt{3}}{2} \alpha_2 \beta_2 - \frac{1}{2} \alpha_1 \beta_3 \end{pmatrix},$$

$$\mathbf{3} \otimes \mathbf{3} = \mathbf{3}' \otimes \mathbf{3}' = \mathbf{1} \oplus \mathbf{2} \oplus \mathbf{3} \oplus \mathbf{3}' \quad (77)$$

$$\mathbf{1} \sim \alpha_1 \beta_1 + \alpha_2 \beta_3 + \alpha_3 \beta_2, \quad \mathbf{2} \sim \begin{pmatrix} \alpha_1 \beta_1 - \frac{1}{2} (\alpha_2 \beta_3 + \alpha_3 \beta_2) \\ \frac{\sqrt{3}}{2} (\alpha_2 \beta_2 + \alpha_3 \beta_3) \end{pmatrix},$$

$$\mathbf{3} \sim \begin{pmatrix} \alpha_3 \beta_3 - \alpha_2 \beta_2 \\ \alpha_1 \beta_3 + \alpha_3 \beta_1 \\ -\alpha_1 \beta_2 - \alpha_2 \beta_1 \end{pmatrix}, \quad \mathbf{3}' \sim \begin{pmatrix} \alpha_3 \beta_2 - \alpha_2 \beta_3 \\ \alpha_2 \beta_1 - \alpha_1 \beta_2 \\ \alpha_1 \beta_3 - \alpha_3 \beta_1 \end{pmatrix},$$

$$\mathbf{3} \otimes \mathbf{3}' = \mathbf{1}' \oplus \mathbf{2} \oplus \mathbf{3} \oplus \mathbf{3}' \quad (78)$$

$$\mathbf{1}' \sim \alpha_1 \beta_1 + \alpha_2 \beta_3 + \alpha_3 \beta_2, \quad \mathbf{2} \sim \begin{pmatrix} \frac{\sqrt{3}}{2} (\alpha_2 \beta_2 + \alpha_3 \beta_3) \\ -\alpha_1 \beta_1 + \frac{1}{2} (\alpha_2 \beta_3 + \alpha_3 \beta_2) \end{pmatrix},$$

$$\mathbf{3} \sim \begin{pmatrix} \alpha_3 \beta_2 - \alpha_2 \beta_3 \\ \alpha_2 \beta_1 - \alpha_1 \beta_2 \\ \alpha_1 \beta_3 - \alpha_3 \beta_1 \end{pmatrix}, \quad \mathbf{3}' \sim \begin{pmatrix} \alpha_3 \beta_3 - \alpha_2 \beta_2 \\ \alpha_1 \beta_3 + \alpha_3 \beta_1 \\ -\alpha_1 \beta_2 - \alpha_2 \beta_1 \end{pmatrix}.$$

The basis in the space of the lowest-weight modular forms can be written in q -expansion as

$$Y_1 = -3\pi \left(\frac{1}{8} + 3q + 3q^2 + 12q^3 + 3q^4 + 18q^5 + 12q^6 + 24q^7 + 3q^8 + 39q^9 \right) ; \quad (79)$$

$$Y_2 = 3\sqrt{3}\pi q^{1/2} (1 + 4q + 6q^2 + 8q^3 + 13q^4 + 12q^5 + 14q^6 + 24q^7 + 18q^8 + 20q^9) ; \quad (80)$$

$$Y_3 = \pi \left(\frac{1}{4} - 2q + 6q^2 - 8q^3 + 6q^4 - 12q^5 + 24q^6 - 16q^7 + 6q^8 - 26q^9 + 38q^{10} \right) ; \quad (81)$$

$$Y_4 = -\sqrt{2}\pi q^{1/4} (1 + 6q + 13q^2 + 14q^3 + 18q^4 + 32q^5 + 31q^6 + 30q^7 + 48q^8 + 38q^9) ; \quad (82)$$

$$Y_5 = -4\sqrt{2}\pi q^{3/4} (1 + 2q + 3q^2 + 6q^3 + 5q^4 + 6q^5 + 10q^6 + 8q^7 + 12q^8 + 14q^9) , \quad (83)$$

where $q \equiv e^{i2\pi\tau}$. The modular-form multiplets of the lowest weight are

$$Y_2 = \begin{pmatrix} Y_1 \\ Y_2 \end{pmatrix}, \quad Y_{\mathbf{3}'} = \begin{pmatrix} Y_3 \\ Y_4 \\ Y_5 \end{pmatrix}. \quad (84)$$

At weight four, the modular-form multiplets are

$$Y_1^{(4)} = Y_1^2 + Y_2^2, \quad Y_2^{(4)} = \begin{pmatrix} Y_2^2 - Y_1^2 \\ 2Y_1Y_2 \end{pmatrix}, \quad (85)$$

$$Y_3^{(4)} = \begin{pmatrix} -2Y_2Y_3 \\ \sqrt{3}Y_1Y_5 + Y_2Y_4 \\ \sqrt{3}Y_1Y_4 + Y_2Y_5 \end{pmatrix}, \quad Y_{\mathbf{3}'}^{(4)} = \begin{pmatrix} 2Y_1Y_3 \\ \sqrt{3}Y_2Y_5 - Y_1Y_4 \\ \sqrt{3}Y_2Y_4 - Y_1Y_5 \end{pmatrix}, \quad (86)$$

where we use superscript “(4)” to explicitly indicate the modular weight.

C Block Diagonalization in ISS(2,3) Models

Block diagonalization in ISS(2,3) models is distinct from that in the $n_{N_R} = n_{S_L}$ ISS models, mainly due to the rectangular matrices M_D and M_S in the former cases. We firstly review the block diagonalization procedure in type-I seesaw [53, 82], which is useful in later discussions.

Consider the full neutrino mass matrix in type-I seesaw with three left-handed and k right-handed neutrinos

$$\begin{pmatrix} \mathbf{0}_{3 \times 3} & [M_D]_{3 \times k} \\ [M_D^\dagger]_{k \times 3} & [M_N]_{k \times k} \end{pmatrix}, \quad (87)$$

which can be block-diagonalized by a unitary matrix like

$$\Omega^T \begin{pmatrix} \mathbf{0}_{3 \times 3} & [M_D]_{3 \times k} \\ [M_D^\dagger]_{k \times 3} & [M_N]_{k \times k} \end{pmatrix} \Omega = \begin{pmatrix} [U \widehat{M}_\nu U^T]_{3 \times 3} & \mathbf{0}_{3 \times k} \\ \mathbf{0}_{k \times 3} & [V \widehat{M}_N V^T]_{k \times k} \end{pmatrix}, \quad (88)$$

where U and V are unitary matrices and $M_\nu = U \widehat{M}_\nu U^T$. With

$$\Omega = \exp \begin{pmatrix} \mathbf{0} & R \\ -R^\dagger & \mathbf{0} \end{pmatrix} = \begin{pmatrix} 1 - \frac{1}{2} R R^\dagger & R \\ -R^\dagger & 1 - \frac{1}{2} R^\dagger R \end{pmatrix} + \mathcal{O}(R^3), \quad (89)$$

we find

$$U \widehat{M}_\nu U^T = -R^* M_N R^\dagger, \quad (90)$$

$$V \widehat{M}_N V^T = M_N + \frac{1}{2} M_N R^\dagger R + \frac{1}{2} R^T R^* M_N. \quad (91)$$

The vanishing non-diagonal entities give

$$R^* = M_D M_N^{-1} . \quad (92)$$

Substituting R in Eq. (90), we find the type-I seesaw formula $M_\nu = -M_D M_N^{-1} M_D^T$.

A full mass matrix in ISS models with $n_{N_R} = n_{S_L}$ is

$$\begin{pmatrix} \mathbf{0} & m_D & \mathbf{0} \\ m_D^T & \mathbf{0} & M_S^T \\ \mathbf{0} & M_S & \mu \end{pmatrix} = \begin{pmatrix} \mathbf{0} & M_D \\ M_D^T & M_N \end{pmatrix} , \quad (93)$$

where we define

$$M_D = (m_D \ \mathbf{0}) , \quad M_N = \begin{pmatrix} \mathbf{0} & M_S^T \\ M_S & \mu \end{pmatrix} . \quad (94)$$

With

$$R^* = M_D M_N^* = -M_S^{-1} \mu (M_S^{-1})^T m_D^T (M_S^{-1})^T m_D^T , \quad (95)$$

we get

$$M_\nu = -R^* M_N R^\dagger = -m_D M_S^{-1} \mu (M_S^{-1})^T m_D^T . \quad (96)$$

Directly applying Eq. (96) to the $n_{N_R} \neq n_{S_L}$ case is not possible as M_S is a rectangular matrix which has no inverse, but the procedure works in the same way. Considering the full mass matrix in Eq. (21) in our model, with

$$M'_D = ([M_D]_{3 \times 2} \ \mathbf{0}_{3 \times 3}) , \quad M'_N = \begin{pmatrix} \mathbf{0}_{2 \times 2} & [M_S^T]_{2 \times 3} \\ [M_S]_{3 \times 2} & [\mu]_{3 \times 3} \end{pmatrix} , \quad (97)$$

we can express the light neutrino mass matrix in the same form as that of type-I seesaw, i.e., $M_\nu = -M'_D (M'_N)^{-1} M_D'^T$. All we need is to find the inverse matrix of M'_N , which does exist

$$M_N'^{-1} = \begin{pmatrix} - \left[(M_S^T M_S M_S^T M_S)^{-1} M_S^T \mu M_S \right]_{2 \times 2} & \left[(M_S^T M_S)^{-1} M_S^T \right]_{2 \times 3} \\ \left[(M_S M_S^T)^{-1} M_S \right]_{3 \times 2} & \mathbf{0}_{3 \times 3} \end{pmatrix}_{5 \times 5} . \quad (98)$$

Substituting M'_D and $M_N'^{-1}$ in Eq. (97) and Eq. (98) into $M_\nu = -M'_D (M'_N)^{-1} M_D'^T$, we get the expression in Eq. (22).

References

- [1] T. Kajita, “Nobel Lecture: Discovery of atmospheric neutrino oscillations,” *Rev. Mod. Phys.* **88**, no.3, 030501 (2016)
- [2] A. B. McDonald, “Nobel Lecture: The Sudbury Neutrino Observatory: Observation of flavor change for solar neutrinos,” *Rev. Mod. Phys.* **88**, no.3, 030502 (2016)
- [3] L. Bergström, “Nonbaryonic dark matter: Observational evidence and detection methods,” *Rept. Prog. Phys.* **63**, 793 (2000) [arXiv:hep-ph/0002126 [hep-ph]].

- [4] G. Bertone, D. Hooper and J. Silk, “Particle dark matter: Evidence, candidates and constraints,” *Phys. Rept.* **405**, 279-390 (2005) [arXiv:hep-ph/0404175 [hep-ph]].
- [5] J. L. Feng, “Dark Matter Candidates from Particle Physics and Methods of Detection,” *Ann. Rev. Astron. Astrophys.* **48**, 495-545 (2010) [arXiv:1003.0904 [astro-ph.CO]].
- [6] G. Bertone and D. Hooper, “History of dark matter,” *Rev. Mod. Phys.* **90**, no. 4, 045002 (2018) [arXiv:1605.04909 [astro-ph.CO]].
- [7] P. Minkowski, “ $\mu \rightarrow e\gamma$ at a Rate of One Out of 10^9 Muon Decays?,” *Phys. Lett. B* **67**, 421-428 (1977)
- [8] R. N. Mohapatra and G. Senjanovic, “Neutrino Mass and Spontaneous Parity Nonconservation,” *Phys. Rev. Lett.* **44**, 912 (1980)
- [9] M. Gell-Mann, P. Ramond and R. Slansky, “Complex Spinors and Unified Theories,” *Conf. Proc. C* **790927**, 315-321 (1979) [arXiv:1306.4669 [hep-th]].
- [10] R. N. Mohapatra and J. W. F. Valle, “Neutrino Mass and Baryon Number Nonconservation in Superstring Models,” *Phys. Rev. D* **34**, 1642 (1986)
- [11] M. C. Gonzalez-Garcia and J. W. F. Valle, “Fast Decaying Neutrinos and Observable Flavor Violation in a New Class of Majoron Models,” *Phys. Lett. B* **216**, 360-366 (1989)
- [12] F. Deppisch and J. W. F. Valle, “Enhanced lepton flavor violation in the supersymmetric inverse seesaw model,” *Phys. Rev. D* **72**, 036001 (2005) [arXiv:hep-ph/0406040 [hep-ph]].
- [13] G. 't Hooft, “Naturalness, chiral symmetry, and spontaneous chiral symmetry breaking,” *NATO Sci. Ser. B* **59**, 135-157 (1980).
- [14] M. Malinsky, J. C. Romao and J. W. F. Valle, “Novel supersymmetric SO(10) seesaw mechanism,” *Phys. Rev. Lett.* **95**, 161801 (2005) [arXiv:hep-ph/0506296 [hep-ph]].
- [15] F. F. Deppisch, P. S. Bhupal Dev and A. Pilaftsis, “Neutrinos and Collider Physics,” *New J. Phys.* **17**, no.7, 075019 (2015) [arXiv:1502.06541].
- [16] M. Malinsky, T. Ohlsson, Z. z. Xing and H. Zhang, “Non-unitary neutrino mixing and CP violation in the minimal inverse seesaw model,” *Phys. Lett. B* **679**, 242-248 (2009) [arXiv:0905.2889].
- [17] A. Abada and M. Lucente, “Looking for the minimal inverse seesaw realisation,” *Nucl. Phys. B* **885**, 651-678 (2014) [arXiv:1401.1507 [hep-ph]].
- [18] S. T. Petcov, “Discrete Flavour Symmetries, Neutrino Mixing and Leptonic CP Violation,” *Eur. Phys. J. C* **78**, no.9, 709 (2018) [arXiv:1711.10806 [hep-ph]].
- [19] S. F. King, “Unified Models of Neutrinos, Flavour and CP Violation,” *Prog. Part. Nucl. Phys.* **94**, 217-256 (2017) [arXiv:1701.04413 [hep-ph]].
- [20] Z. z. Xing, “Flavor structures of charged fermions and massive neutrinos,” *Phys. Rept.* **854**, 1-147 (2020) [arXiv:1909.09610 [hep-ph]].
- [21] F. Feruglio, “Are neutrino masses modular forms?,” [arXiv:1706.08749 [hep-ph]].

- [22] J. T. Penedo and S. T. Petcov, “Lepton Masses and Mixing from Modular S_4 Symmetry,” Nucl. Phys. B **939**, 292-307 (2019) [arXiv:1806.11040 [hep-ph]].
- [23] P. P. Novichkov, J. T. Penedo, S. T. Petcov and A. V. Titov, “Modular S_4 models of lepton masses and mixing,” JHEP **04**, 005 (2019) [arXiv:1811.04933 [hep-ph]].
- [24] P. P. Novichkov, J. T. Penedo, S. T. Petcov and A. V. Titov, “Generalised CP Symmetry in Modular-Invariant Models of Flavour,” JHEP **07**, 165 (2019) [arXiv:1905.11970 [hep-ph]].
- [25] H. Okada and Y. Orikasa, “Neutrino mass model with a modular S_4 symmetry,” [arXiv:1908.08409 [hep-ph]].
- [26] S. F. King and Y. L. Zhou, “Trimaximal TM_1 mixing with two modular S_4 groups,” Phys. Rev. D **101**, no.1, 015001 (2020) [arXiv:1908.02770 [hep-ph]].
- [27] J. C. Criado, F. Feruglio and S. J. D. King, “Modular Invariant Models of Lepton Masses at Levels 4 and 5,” JHEP **02**, 001 (2020) [arXiv:1908.11867 [hep-ph]].
- [28] X. Wang and S. Zhou, “The minimal seesaw model with a modular S_4 symmetry,” JHEP **05**, 017 (2020) [arXiv:1910.09473 [hep-ph]].
- [29] G. J. Ding, S. F. King, X. G. Liu and J. N. Lu, “Modular S_4 and A_4 symmetries and their fixed points: new predictive examples of lepton mixing,” JHEP **12**, 030 (2019) [arXiv:1910.03460 [hep-ph]].
- [30] M. Hirsch, S. Morisi and J. W. F. Valle, “ A_4 -based tri-bimaximal mixing within inverse and linear seesaw schemes,” Phys. Lett. B **679**, 454-459 (2009) [arXiv:0905.3056 [hep-ph]].
- [31] P. S. B. Dev and R. N. Mohapatra, “TeV Scale Inverse Seesaw in $SO(10)$ and Leptonic Non-Unitarity Effects,” Phys. Rev. D **81**, 013001 (2010) [arXiv:0910.3924 [hep-ph]].
- [32] A. Abada, M. E. Krauss, W. Porod, F. Staub, A. Vicente and C. Weiland, “Lepton flavor violation in low-scale seesaw models: SUSY and non-SUSY contributions,” JHEP **11**, 048 (2014) [arXiv:1408.0138 [hep-ph]].
- [33] S. Centelles Chuliá, R. Srivastava and A. Vicente, “The inverse seesaw family: Dirac and Majorana,” JHEP **03**, 248 (2021) [arXiv:2011.06609 [hep-ph]].
- [34] H. B. Camara, R. G. Felipe and F. R. Joaquim, “Minimal inverse-seesaw mechanism with Abelian flavour symmetries,” JHEP **05**, 021 (2021) [arXiv:2012.04557 [hep-ph]].
- [35] T. Nomura, H. Okada and S. Patra, “An inverse seesaw model with A_4 -modular symmetry,” Nucl. Phys. B **967**, 115395 (2021) [arXiv:1912.00379 [hep-ph]].
- [36] T. Nomura and H. Okada, “Modular A_4 symmetric inverse seesaw model with $SU(2)_L$ multiplet fields,” [arXiv:2007.15459 [hep-ph]].
- [37] S. A. R. Ellis, K. J. Kelly and S. W. Li, “Current and Future Neutrino Oscillation Constraints on Leptonic Unitarity,” JHEP **12**, 068 (2020) [arXiv:2008.01088 [hep-ph]].
- [38] F. Feroz and M. P. Hobson, “Multimodal nested sampling: an efficient and robust alternative to MCMC methods for astronomical data analysis,” Mon. Not. Roy. Astron. Soc. **384**, 449 (2008) [arXiv:0704.3704 [astro-ph]].

- [39] F. Feroz, M. P. Hobson and M. Bridges, “MultiNest: an efficient and robust Bayesian inference tool for cosmology and particle physics,” *Mon. Not. Roy. Astron. Soc.* **398**, 1601-1614 (2009) [arXiv:0809.3437 [astro-ph]].
- [40] F. Feroz, M. P. Hobson, E. Cameron and A. N. Pettitt, “Importance Nested Sampling and the MultiNest Algorithm,” *Open J. Astrophys.* **2**, no.1, 10 (2019) [arXiv:1306.2144 [astro-ph.IM]].
- [41] G. y. Huang and S. Zhou, “Precise Values of Running Quark and Lepton Masses in the Standard Model,” *Phys. Rev. D* **103**, no.1, 016010 (2021) [arXiv:2009.04851 [hep-ph]].
- [42] I. Esteban, M. C. Gonzalez-Garcia, M. Maltoni, T. Schwetz and A. Zhou, “The fate of hints: updated global analysis of three-flavor neutrino oscillations,” *JHEP* **09**, 178 (2020) [arXiv:2007.14792 [hep-ph]]. NuFIT 5.0 (2020), www.nu-fit.org.
- [43] A. Lewis, “GetDist: a Python package for analysing Monte Carlo samples,” [arXiv:1910.13970 [astro-ph.IM]].
- [44] F. Capozzi, E. Di Valentino, E. Lisi, A. Marrone, A. Melchiorri and A. Palazzo, “Global constraints on absolute neutrino masses and their ordering,” *Phys. Rev. D* **95**, no.9, 096014 (2017) [arXiv:2003.08511 [hep-ph]].
- [45] S. Tremaine and J. E. Gunn, “Dynamical Role of Light Neutral Leptons in Cosmology,” *Phys. Rev. Lett.* **42**, 407-410 (1979)
- [46] S. Dodelson and L. M. Widrow, “Sterile-neutrinos as dark matter,” *Phys. Rev. Lett.* **72**, 17-20 (1994) [arXiv:hep-ph/9303287 [hep-ph]].
- [47] X. D. Shi and G. M. Fuller, “A New dark matter candidate: Nonthermal sterile neutrinos,” *Phys. Rev. Lett.* **82**, 2832-2835 (1999) [arXiv:astro-ph/9810076 [astro-ph]].
- [48] L. Wolfenstein, “Neutrino Oscillations in Matter,” *Phys. Rev. D* **17**, 2369-2374 (1978)
- [49] S. P. Mikheyev and A. Y. Smirnov, “Resonance Amplification of Oscillations in Matter and Spectroscopy of Solar Neutrinos,” *Sov. J. Nucl. Phys.* **42**, 913-917 (1985)
- [50] S. P. Mikheev and A. Y. Smirnov, “Resonant amplification of neutrino oscillations in matter and solar neutrino spectroscopy,” *Nuovo Cim. C* **9**, 17-26 (1986)
- [51] K. Abazajian, G. M. Fuller and M. Patel, “Sterile neutrino hot, warm, and cold dark matter,” *Phys. Rev. D* **64**, 023501 (2001) [arXiv:astro-ph/0101524 [astro-ph]].
- [52] A. Kusenko, “Sterile neutrinos: The Dark side of the light fermions,” *Phys. Rept.* **481**, 1-28 (2009) [arXiv:0906.2968 [hep-ph]].
- [53] A. Merle, “keV Neutrino Model Building,” *Int. J. Mod. Phys. D* **22**, 1330020 (2013) [arXiv:1302.2625 [hep-ph]].
- [54] A. Merle, “Sterile Neutrino Dark Matter,” Morgan & Claypool Publishers, 2053-2571 Mar (2017)
- [55] K. N. Abazajian, “Sterile neutrinos in cosmology,” *Phys. Rept.* **711-712**, 1-28 (2017) [arXiv:1705.01837 [hep-ph]].

- [56] N. Aghanim *et al.* [Planck], “Planck 2018 results. VI. Cosmological parameters,” *Astron. Astrophys.* **641**, A6 (2020) [arXiv:1807.06209 [astro-ph.CO]].
- [57] T. Asaka, M. Laine and M. Shaposhnikov, “Lightest sterile neutrino abundance within the nuMSM,” *JHEP* **01**, 091 (2007) [erratum: *JHEP* **02**, 028 (2015)] [arXiv:hep-ph/0612182 [hep-ph]].
- [58] S. Horiuchi, P. J. Humphrey, J. Onorbe, K. N. Abazajian, M. Kaplinghat and S. Garrison-Kimmel, “Sterile neutrino dark matter bounds from galaxies of the Local Group,” *Phys. Rev. D* **89**, no.2, 025017 (2014) [arXiv:1311.0282 [astro-ph.CO]].
- [59] D. Malyshev, A. Neronov and D. Eckert, “Constraints on 3.55 keV line emission from stacked observations of dwarf spheroidal galaxies,” *Phys. Rev. D* **90**, 103506 (2014) [arXiv:1408.3531 [astro-ph.HE]].
- [60] B. M. Roach, K. C. Y. Ng, K. Perez, J. F. Beacom, S. Horiuchi, R. Krivonos and D. R. Wik, “NuSTAR Tests of Sterile-Neutrino Dark Matter: New Galactic Bulge Observations and Combined Impact,” *Phys. Rev. D* **101**, no.10, 103011 (2020) [arXiv:1908.09037 [astro-ph.HE]].
- [61] M. Viel, G. D. Becker, J. S. Bolton and M. G. Haehnelt, “Warm dark matter as a solution to the small scale crisis: New constraints from high redshift Lyman- α forest data,” *Phys. Rev. D* **88**, 043502 (2013) [arXiv:1306.2314 [astro-ph.CO]].
- [62] J. Baur, N. Palanque-Delabrouille, C. Yèche, C. Magneville and M. Viel, “Lyman-alpha Forests cool Warm Dark Matter,” *JCAP* **08**, 012 (2016) [arXiv:1512.01981 [astro-ph.CO]].
- [63] V. Iršič, M. Viel, M. G. Haehnelt, J. S. Bolton, S. Cristiani, G. Cupani, T. S. Kim, V. D’Odorico, S. López and S. Ellison, *et al.* “New Constraints on the free-streaming of warm dark matter from intermediate and small scale Lyman- α forest data,” *Phys. Rev. D* **96**, no.2, 023522 (2017) [arXiv:1702.01764 [astro-ph.CO]].
- [64] N. Palanque-Delabrouille, C. Yèche, N. Schöneberg, J. Lesgourgues, M. Walther, S. Chabanier and E. Armengaud, “Hints, neutrino bounds and WDM constraints from SDSS DR14 Lyman- α and Planck full-survey data,” *JCAP* **04**, 038 (2020) [arXiv:1911.09073 [astro-ph.CO]].
- [65] A. Garzilli, O. Ruchayskiy, A. Magalich and A. Boyarsky, “How warm is too warm? Towards robust Lyman- α forest bounds on warm dark matter,” [arXiv:1912.09397 [astro-ph.CO]].
- [66] J. F. Cherry and S. Horiuchi, “Closing in on Resonantly Produced Sterile Neutrino Dark Matter,” *Phys. Rev. D* **95**, no.8, 083015 (2017) [arXiv:1701.07874 [hep-ph]].
- [67] A. D. Dolgov, S. H. Hansen, G. Raffelt and D. V. Semikoz, “Heavy sterile neutrinos: Bounds from big bang nucleosynthesis and SN1987A,” *Nucl. Phys. B* **590**, 562-574 (2000) [arXiv:hep-ph/0008138 [hep-ph]].
- [68] G. G. Raffelt and S. Zhou, “Supernova bound on keV-mass sterile neutrinos reexamined,” *Phys. Rev. D* **83**, 093014 (2011) [arXiv:1102.5124 [hep-ph]].
- [69] S. Zhou, “Supernova Bounds on keV-mass Sterile Neutrinos,” *Int. J. Mod. Phys. A* **30**, no.13, 1530033 (2015) [arXiv:1504.02729 [hep-ph]].
- [70] C. A. Argüelles, V. Brdar and J. Kopp, “Production of keV Sterile Neutrinos in Supernovae: New Constraints and Gamma Ray Observables,” *Phys. Rev. D* **99**, no.4, 043012 (2019) [arXiv:1605.00654 [hep-ph]].

- [71] A. M. Suliga, I. Tamborra and M. R. Wu, “Lifting the core-collapse supernova bounds on keV-mass sterile neutrinos,” JCAP **08**, 018 (2020) [arXiv:2004.11389 [astro-ph.HE]].
- [72] M. Hirsch, T. Kernreiter, J. C. Romao and A. Villanova del Moral, “Minimal Supersymmetric Inverse Seesaw: Neutrino masses, lepton flavour violation and LHC phenomenology,” JHEP **01**, 103 (2010) [arXiv:0910.2435 [hep-ph]].
- [73] A. Das and N. Okada, “Inverse seesaw neutrino signatures at the LHC and ILC,” Phys. Rev. D **88**, 113001 (2013) [arXiv:1207.3734 [hep-ph]].
- [74] P. Bandyopadhyay, E. J. Chun, H. Okada and J. C. Park, “Higgs Signatures in Inverse Seesaw Model at the LHC,” JHEP **01**, 079 (2013) [arXiv:1209.4803 [hep-ph]].
- [75] A. Das, P. S. Bhupal Dev and N. Okada, “Direct bounds on electroweak scale pseudo-Dirac neutrinos from $\sqrt{s} = 8$ TeV LHC data,” Phys. Lett. B **735**, 364-370 (2014) [arXiv:1405.0177 [hep-ph]].
- [76] A. Das and N. Okada, “Improved bounds on the heavy neutrino productions at the LHC,” Phys. Rev. D **93**, no.3, 033003 (2016) [arXiv:1510.04790 [hep-ph]].
- [77] A. Das, S. Jana, S. Mandal and S. Nandi, “Probing right handed neutrinos at the LHeC and lepton colliders using fat jet signatures,” Phys. Rev. D **99**, no.5, 055030 (2019) [arXiv:1811.04291 [hep-ph]].
- [78] B. Bozek, M. Boylan-Kolchin, S. Horiuchi, S. Garrison-Kimmel, K. Abazajian and J. S. Bullock, “Resonant Sterile Neutrino Dark Matter in the Local and High- z Universe,” Mon. Not. Roy. Astron. Soc. **459**, no.2, 1489-1504 (2016) [arXiv:1512.04544 [astro-ph.CO]].
- [79] F. Bezrukov, H. Hettmansperger and M. Lindner, “keV sterile neutrino Dark Matter in gauge extensions of the Standard Model,” Phys. Rev. D **81**, 085032 (2010) [arXiv:0912.4415 [hep-ph]].
- [80] A. Abada, G. Arcadi and M. Lucente, “Dark Matter in the minimal Inverse Seesaw mechanism,” JCAP **10**, 001 (2014) [arXiv:1406.6556 [hep-ph]].
- [81] J. Baur, N. Palanque-Delabrouille, C. Yèche, A. Boyarsky, O. Ruchayskiy, É. Armengaud and J. Lesgourgues, “Constraints from Ly- α forests on non-thermal dark matter including resonantly-produced sterile neutrinos,” JCAP **12**, 013 (2017) [arXiv:1706.03118 [astro-ph.CO]].
- [82] A. Ibarra, E. Molinaro and S. T. Petcov, “TeV Scale See-Saw Mechanisms of Neutrino Mass Generation, the Majorana Nature of the Heavy Singlet Neutrinos and $(\beta\beta)_{0\nu}$ -Decay,” JHEP **09**, 108 (2010) [arXiv:1007.2378 [hep-ph]].